National Library of Canada

Acquisitions and Bibliographic Services Branch

395 Wellington Street
Ottawa, Ontario
K1A 0N4

Bibliothèque nationale du Canada

Direction des acquisitions et des services bibliographiques

395, rue Wellington
Ottawa (Ontario)
K1A 0N4

Your file Votre référence

Our file Notre référence

NOTICE

The quality of this microform is heavily dependent upon the quality of the original thesis submitted for microfilming. Every effort has been made to ensure the highest quality of reproduction possible.

If pages are missing, contact the university which granted the degree.

Some pages may have indistinct print especially if the original pages were typed with a poor typewriter ribbon or if the university sent us an inferior photocopy.

Reproduction in full or in part of this microform is governed by the Canadian Copyright Act, R.S.C. 1970, c. C-30, and subsequent amendments.

AVIS

La qualité de cette microforme dépend grandement de la qualité de la thèse soumise au microfilmage. Nous avons tout fait pour assurer une qualité supérieure de reproduction.

S'il manque des pages, veuillez communiquer avec l'université qui a conféré le grade.

La qualité d'impression de certaines pages peut laisser à désirer, surtout si les pages originales ont été dactylographiées à l'aide d'un ruban usé ou si l'université nous a fait parvenir une photocopie de qualité inférieure.

La reproduction, même partielle, de cette microforme est soumise à la Loi canadienne sur le droit d'auteur, SRC 1970, c. C-30, et ses amendements subséquents.

Canada

UNIVERSITY OF ALBERTA

Structural Geology of the Triangle Zone at Langford Creek, S.W. Alberta.

by

Byron Veilleux

A Thesis submitted to the Faculty of Graduate Studies and Research in partial fulfilment of the requirements for the degree of Master of Science.

Department of Geology

Edmonton, Alberta

Spring, 1993

National Library
of Canada

Acquisitions and
Bibliographic Services Branch

395 Wellington Street
Ottawa, Ontario
K1A 0N4

Bibliothèque nationale
du Canada

Direction des acquisitions et
des services bibliographiques

395, rue Wellington
Ottawa (Ontario)
K1A 0N4

Your file Votre référence

Our file Notre référence

The author has granted an irrevocable non-exclusive licence allowing the National Library of Canada to reproduce, loan, distribute or sell copies of his/her thesis by any means and in any form or format, making this thesis available to interested persons.

L'auteur a accordé une licence irrévocable et non exclusive permettant à la Bibliothèque nationale du Canada de reproduire, prêter, distribuer ou vendre des copies de sa thèse de quelque manière et sous quelque forme que ce soit pour mettre des exemplaires de cette thèse à la disposition des personnes intéressées.

The author retains ownership of the copyright in his/her thesis. Neither the thesis nor substantial extracts from it may be printed or otherwise reproduced without his/her permission.

L'auteur conserve la propriété du droit d'auteur qui protège sa thèse. Ni la thèse ni des extraits substantiels de celle-ci ne doivent être imprimés ou autrement reproduits sans son autorisation.

ISBN 0-315-88109-7

Canada

UNIVERSITY OF ALBERTA

RELEASE FORM

NAME OF AUTHOR: Byron Veilleux

TITLE OF THESIS: Structural Geology of the Triangle Zone at Langford Creek, S. W. Alberta.

DEGREE FOR WHICH THESIS WAS PRESENTED: Master of Science:

YEAR THIS DEGREE GRANTED: Spring, 1993

Permission is hereby granted to THE UNIVERSITY OF ALBERTA LIBRARY to reproduce single copies of this thesis and to lend or sell such copies for private, scholarly or scientific research purposes only.

The author reserves all other publication and other rights in association with the copyright in the thesis, and except as hereinbefore provided neither the thesis nor any substantial portion thereof may be printed or otherwise reproduced in any material form whatever without the author's prior written permission.

2827-41st. Street, S. W.

Calgary, Alberta

T3E 3K7

Date January 5, 1993

THE UNIVERSITY OF ALBERTA

FACULTY OF GRADUATE STUDIES AND RESEARCH

The undersigned certify that they have read, and recommend to Faculty of Graduate Studies and Research, for acceptance, a thesis entitled Structural Geology of the Triangle Zone at Langford Creek, S. W. Alberta submitted by Byron W. Veilleux in partial fulfilment of the requirements for the degree of Master of Science in Geology.

H.A.K. Charlesworth

Dr. H.A.K. Charlesworth

Philippe Erdmer

Dr. P. Erdmer

Dr. E. Nyland

Dr. D. Cruden

Date January 5, 1992

ABSTRACT

Outcrop and drillhole data within the Langford Creek study area were digitized from Geological Survey of Canada maps and field data, and entered into the computer program TRIPOD. Statistical analysis of outcrops within cylindrically folded domains was conducted to determine fold axes. Outcrops and drillholes within each domain were projected axially onto cross sections using TRIPOD. Seismic data were used to complete three balanced cross sections from these data.

The basal detachment beneath some of the study area lies within the Mississippian Exshaw Formation; elsewhere it is in the Jurassic Fernie Formation. Strata above the upper detachment are cut by a series of foreland-verging thrusts that flatten in an upper detachment situated in the Upper Cretaceous Bearpaw Formation. Strata above this detachment lie in the west limb of the Alberta syncline. The balanced cross-sections provide evidence for a major lateral ramp affecting strata beneath the upper detachment and connecting flats in the Exshaw and Fernie Formations. This structure is responsible for a 5° to 15° southerly plunge of folds at the surface. Displacement associated with foreland verging thrusts below the upper detachment in part continues into the foreland to be dissipated by layer parallel shortening in units above the upper detachment, and in part is transferred to the surface along hinterland verging thrusts.

ACKNOWLEDGEMENTS

This project was first suggested by Dr. H.A.K. Charlesworth. His patience, guidance and kindness throughout the project are gratefully acknowledged. The geologic and geophysical staff of Husky Resources, in particular Kel Johnston and Bill Rennie, provided access to seismic and drillhole data, assistance with the reproduction of figures and helpful discussion throughout the project. Dr. P. Erdmer, who granted access to his structural lab and guidance during Dr. Charlesworth's absences is thanked. Peter Jahans and Dan Bulat are thanked for their time and assistance drafting figures and their companionship and helpful discussions throughout.

Financial support was provided by the University of Alberta by means of a graduate teaching assistantship and a summer research assistantship. Other financial support included a Natural Sciences and Engineering Research Council of Canada operating grant to Dr. Charlesworth.

Many thanks to Rob, Vip, Marc, Jeff, Tracy and many others who joined me in hours of productive research in the Power Plant, I will never forget the laughter and discussions. Finally, I would like to thank my family for all of the support and patience provided during what must have seemed like an endless education process.

TABLE OF CONTENTS

Chapter	Page
CHAPTER 1	1
INTRODUCTION	1
Regional geologic setting and purpose of study	1
Location, accessibility, and exposure	2
Physiography	2
Previous Work	2
CHAPTER 2	6
STRATIGRAPHY	6
Introduction	6
Description of units	6
Thickness determination	12
CHAPTER 3	13
STRUCTURAL GEOLOGY AND SETTING	13
CHAPTER 4	18
DATA COLLECTION, ANALYSIS AND STORAGE	18
Collection and storage of outcrop and drillhole data	18
Analysis of outcrop and drillhole data	22
CHAPTER 5	26
SEISMIC DATA	26
Seismic processing and interpretation	26

Chapter Page

CHAPTER 6 33
MAP AND CROSS SECTION CONSTRUCTION 33
Geologic maps 33
Cross sections 33

CHAPTER 7 36
STRUCTURE 36
Introduction 36
Mississippian to Belly River structure 36
Bearpaw structure 46
Structure of the St. Mary River and younger Formations 48
Structural synthesis 56

CHAPTER 8 58
SUMMARY AND CONCLUSIONS 58

REFERENCES 59
APPENDIX 1 65
APPENDIX 2: 68
APPENDIX 3 81

LIST OF FIGURES

Figure — Page

Figure 1: Location of the Langford Creek Study Area. 3

Figure 2: Map of Langford Creek study area 4

Figure 3: a-c) Three main types of fold-thrust relationships encountered in the Rocky Mountains (From Jamison, 1987). d) Thrusting with layer parallel shortening; shortening is accomplished by development of solution cleavage, mesoscopic deformation, pressure solution assisted grain boundary sliding and other effects (modified from Hatcher et al, 1989). 14

Figure 4: a) Block diagram of lateral, oblique and frontal ramps and related folds. b) Tear fault; displacement along the thrust fault terminates abruptly at strike-slip faults (From Hatcher, 1990). 14

Figure 5: Idealized Triangle Zone - Hinterland dipping, foreland verging thrusts are wedged below the foreland dipping upper detachment surface. 16

Figure 6: Early interpretations of the structure of the triangle zone. 17

Figure 7: Selected UTM points (P_1, P_2) on the 1:50000 contour maps are measured relative to lines of latitude and longitude. These values (xa, ya, xb, yb) are multiplied by the Scale Factor (0.7891414) to give the appropriate distance on the 1:63360 map (xa * 0.7891414 = nx; xb * 0.7891414 = ny). 19

Figure 8: Map of domain boundaries within the Langford Creek study area. 23

Figure 9: Map showing positions of seismic lines used in this study 27

Figure 10: Wave reflected from a horizontal interface, with constant velocity (V_1) between the source and interface. 28

Figure 11: Ray path trajectories and time-distance relationships for a dipping bed. 29

Figure 12: Geometrical relationships used to determine the correct position and dip (θ) of and apparent reflector with a dip of ß. 31

Figure 13: Map showing the position of cross sections 1, 2 and 3. 37

Figure 14: Cross Section 1 - 1'. . . . . in pocket

Figure 15: Seismic Section CAN-WC-1. . . . . in pocket

Figure 16: Schematic section of the Chimney Rock thrust-sheet, Whaleback duplex and incipient Rice Creek thrust. 39

Figure 17: Schematic cross section of the Rice Creek thrust, folded Chimney Rock thrust, Whaleback duplex and incipient Rocking P thrust. 39

Figure 18: Schematic cross sections: a) Stage 1 (ramp stage) formation of the Rocking P horse, the incipient path for stage 2 of the Rocking P thrust. b) Stage 2 of the Rocking P thrust and the Cougar duplex. 40

Figure 19: Cross Section 2 - 2'. . . . . in pocket

Figure 20: Seismic Section CAN-WC-2. . . . . in pocket

Figure 21: Schematic cross sections. a) The Rocking P thrust with folded Rice Creek and incipient YL thrusts. b) The YL thrust and Cougar duplex with the folded Rocking P thrust. 42

Figure 22: Cross Section 3 - 3'. . . . . in pocket

Figure 23: Seismic Section CAN-WC-5. . . . . in pocket

Figure 24: Schematic cross section of the Chimney Rock thrust-sheet and Whaleback duplex with the incipient Rocking P thrust. 44

Figure 25: Map showing the hangingwall cut-off for Mississippian strata (shaded blue) and the position of the footwall ramps to the Rocking P and YL thrusts. 45

Figure 26: a) Incipient geometry of the lateral ramp formed where the Rocking P thrust ramps up-section to the south from the level of the Exshaw Formation to the top of the Fernie Formation. b) Translation of strata above the Rocking P fault over the lateral ramp results in the formation of a lateral ramp anticline with a southerly plunge. The approximate positions of cross sections 1 and 2 are shown. c) The YL thrust transports Mississippian strata to the top of the Fernie Formation, reactivating the Rocking P fault on section 1 (active fault surfaces are shaded grey). The lateral ramp for simplicity is shown as vertical but likely dips to the north at approximately 15°. 47

Figure 27: Map showing locations of plates 2 through 6 and vergence direction (Arrows) evident from mesoscopic structures at each location. 48

Figure 28: Schematic diagram of initial stages of structural thickening within the upper detachment zone. Displacement in strata above the upper detachment is dissipated by layer parallel shortening giving the upper detachment foreland vergence. 57

Figure 29: Schematic section of later stages of structural thickening within the upper detachment zone, with displacement transferred to the surface along a hinterland verging thrust. Diagram shows the approximate position of drillholes within the study area, relative to the outcrop trace of the upper detachment. Structural thickening of Bearpaw formation strata within these wells decreases eastward. 57

Figure 30: Restored cross section 1 1'. . . . . in pocket

Figure 31: Restored cross section 2 2'. . . . . in pocket

Figure 32: Restored cross section 3 3'. . . . . in pocket

LIST OF TABLES

Table Page

Table 1: Table of Formations (Modified from MacKay, 1991). 7

Table 2: Summary of domain analyses and resulting projection directions used to construct geologic cross sections. 24

LIST OF PLATES

Plate — Page

Plate 1: East dipping Upper Cretaceous (St. Mary River Formation) and Tertiary (Porcupine Hills and Willow Creek Formations) strata in the hangingwall of the upper detachment. 49

Plate 2: Faulted anticline in sandstones and shales of the Bearpaw Formation. 51

Plate 3: Asymmetric anticline developed in shales and ironstones of the Bearpaw Formation. 52

Plate 4: Fault propagation fold developed in interbedded ironstone, shale and coal of the basal St. Mary River Formation. 53

Plate 5: Minor structure developed on the east limb of the fault propagation fold of plate 4. 54

Plate 6: Asymmetric anticline developed in strata of the basal St. Mary River Formation. 55

CHAPTER 1
INTRODUCTION

Regional geologic setting and purpose of study

The outer margin of the Rocky Mountain Fold and Thrust belt has been studied extensively since the earliest period of exploration and mapping in the Western Canada Sedimentary Basin. The discovery of oil and gas in the Turner Valley anticline in the early part of the twentieth century resulted in extensive drilling and geologic mapping of the Foothills of southern Alberta. Most petroleum exploration was unsuccessful due to the complex and poorly understood structure. The strata in the Rocky Mountain Fold and Thrust belt were deformed from the Late Jurassic to the Early Tertiary. The outer margin of the belt at the surface is commonly characterized by an east dipping thrust, separating east dipping strata in the Alberta Syncline from dominantly west dipping strata of the Foothills belt. Beneath and to the west of this thrust is the triangle zone. The purpose of this study was to use outcrop, drillhole and seismic data to investigate the structure of the triangle zone immediately south of the Chain Lakes Reservoir in southwestern Alberta. A clearer understanding of the triangle zone will lead to a better understanding of earlier stages of deformation in fold and thrust belts because most thrusts likely initiated in a similar setting. In addition, this area was selected because folds in Mesozoic strata at the surface plunge at 5° to 15° to the south, possibly related to a lateral ramp at depth.

Outcrop data were obtained from Geological Survey of Canada 1:50 000 scale maps and from field work conducted in the fall of 1991. Drillhole data which included dipmeter, deviation and geophysical logs were supplied by Husky Resources Limited of Calgary, Alberta. These data were digitized, outcrop data being placed in the database CHAIN and drillhole data in the database WELLS. Five 24-fold seismic lines were supplied by Husky Resources. These data were used to construct 3 balanced geologic cross-sections through the study area.

Location, accessibility, and exposure

The 1100 km^2 study area is located approximately 100 km south of Calgary, Alberta in NTS 1:50 000 map sheets 82J/1 and 82G/16. It lies between longitudes 114° 30' and 114° 0'W and latitudes 49° 50' and 50° 15'N, immediately south of the Chain Lakes Reservoir (Figure 1). Highway 922 is a recently paved road through the middle of the area. Secondary service roads branch off east and west from Highway 922 and allow access to within approximately 1 km of most locations. Most of the land in the study area is privately owned or is Crown land leased to local ranchers. Most ranchers will readily grant access for workers on foot. Bedrock exposure is moderate to fair along the top of ridges, poor to moderate along creeks and almost non-existent on valley floors.

Physiography

The topography consists of gentle grass covered hills with modest tree cover of Limber Pine, Lodgepole Pine and Buckbrush. Topographic relief is less than 500 m. A broad, flat, northerly trending valley, occupied by the Chain Lakes Reservoir in the north, divides the study area roughly in half (Figure 2). To the east of this valley are the Porcupine Hills, underlain by relatively undeformed east dipping Tertiary strata. Immediately to the west of this valley, an east dipping panel of resistant Upper Cretaceous strata forms the boundary between the west limb of the Alberta syncline and dominantly west dipping Jurassic through Upper Cretaceous strata forming the foothills to the west (Douglas, 1950).

Previous Work

Mapping of the Callum Creek, Langford Creek and Gap map areas was conducted by the Geological Survey of Canada in the late 1940s and 1950s (Douglas, 1950; Norris, 1958). G.S.C. Memoir 255 (Douglas, 1950) was a landmark publication which illustrated many of the deformation mechanisms that are commonly applied to the interpretation of foreland fold and thrust belts at

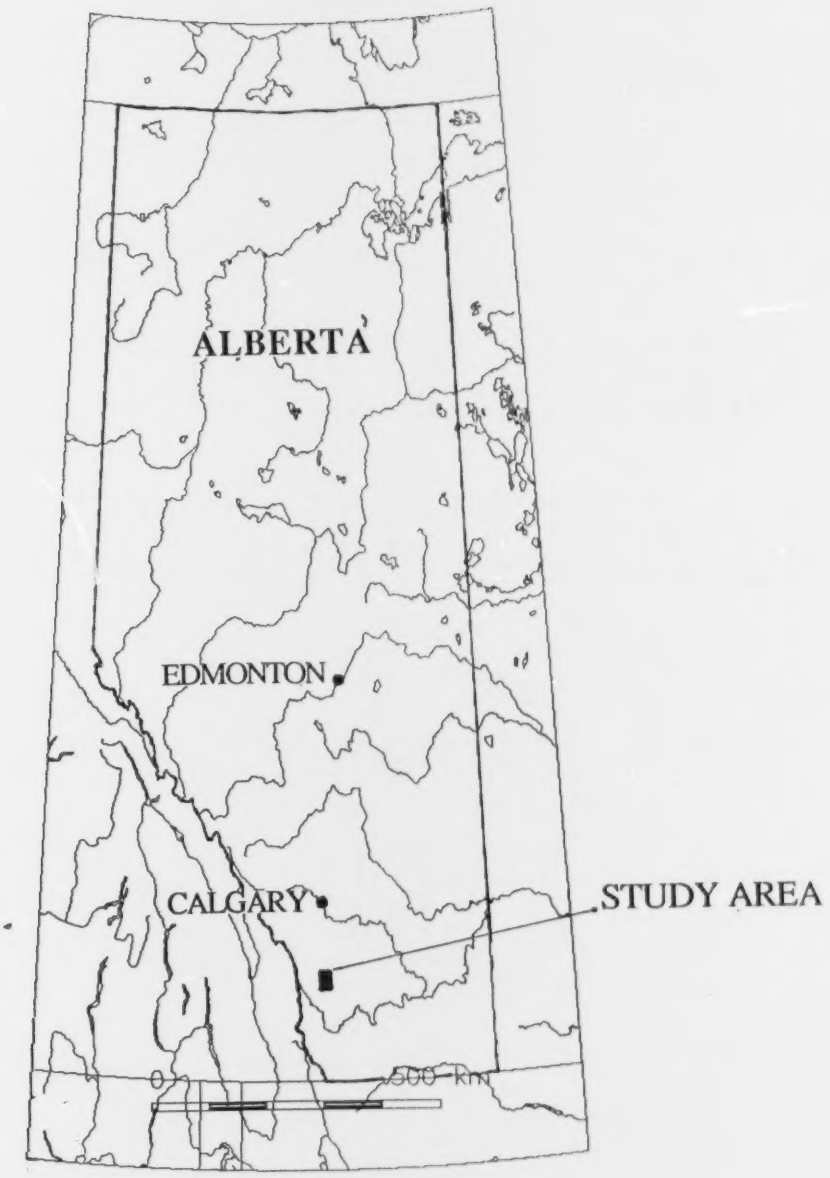

Figure 1: Location of the Langford Creek Study Area.

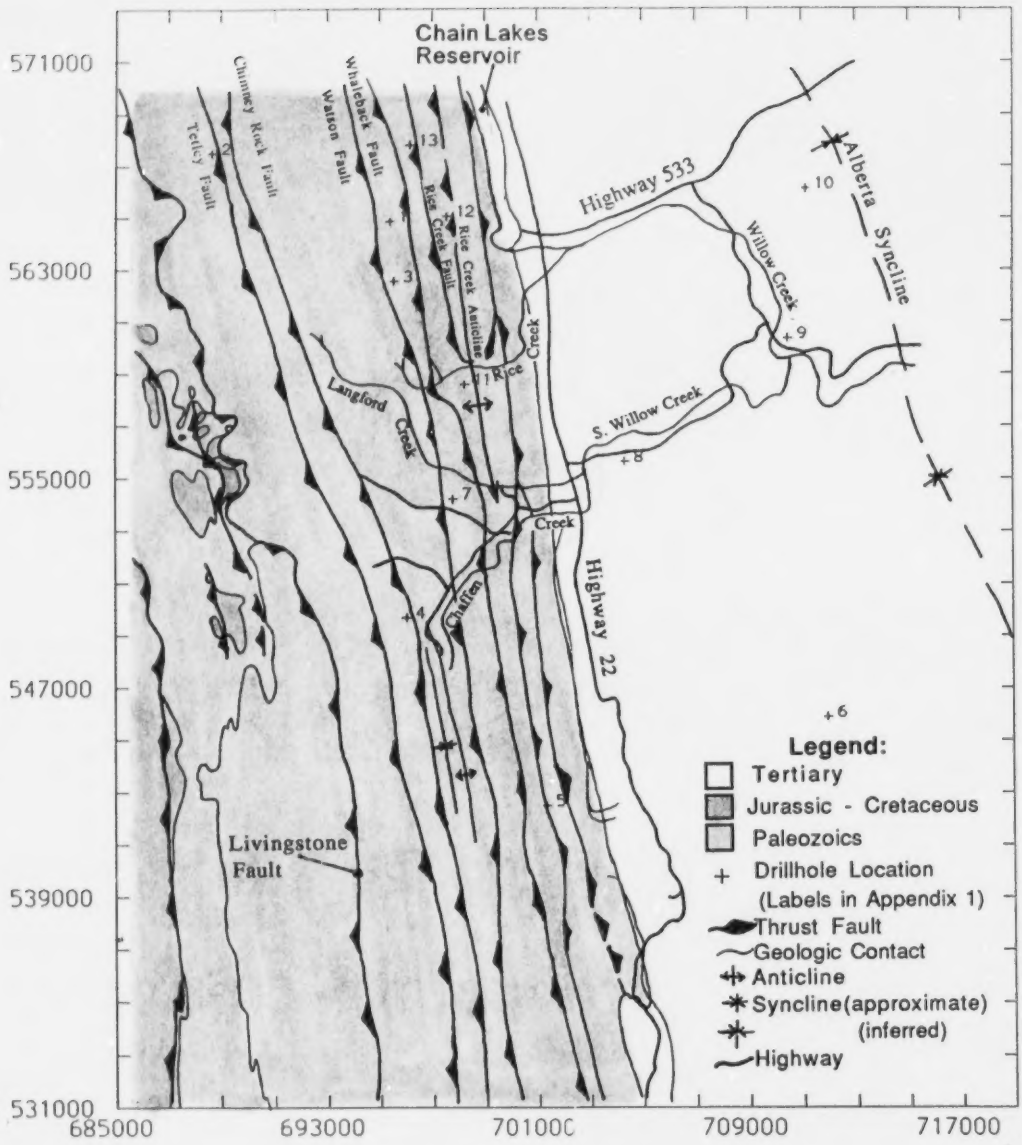

Figure 2: Map of Langford Creek study area, modified after Douglas (1950). The east and west limits of the study area roughly coincide with the axial trace of the Alberta Syncline and the trace of the Livingstone Fault. Grid labels are UTM coordinates in metres. See Appendix 1 for drillhole identifiers.

present. The memoir documented the propagation of thrusts along ramps and bedding parallel flats, as well as the folding of older thrusts by lower, younger thrusts at deeper structural levels.

CHAPTER 2
STRATIGRAPHY

Introduction

Deformed strata in the Rocky Mountain Fold and Thrust Belt may be divided into two distinct stratigraphic packages (Table 1): the miogeoclinal or platform strata and the foreland basin or clastic wedge. The miogeoclinal sequence is dominated by passive margin platform carbonates, lesser clastics and their basinal equivalents. These passive margin strata are Early Paleozoic through Middle Jurassic in age. The foreland basin strata are predominantly synorogenic clastics, derived mainly from a southwesterly source. These strata are Late Jurassic through Paleocene in age, and are related to uplift and deformation to the southwest.

Description of units

Cambrian and Devonian

Cambrian strata, encountered in well #6 (Figure 2), consist of varicoloured, interbedded limestones, dolostones, mature quartz arenites and mixed clastic rocks. Devonian strata of the Palliser Formation and Fairholme Group, approximately 460 m thick, were encountered in this well. They consist of a complex series of platform carbonates, evaporites and lesser clastics of Late Devonian age. Minor, mixed carbonate-clastic strata occur at the base. Cambrian and Devonian strata were deposited on a broad stable carbonate platform (Aitken, 1989). Cambrian and Devonian strata within the study area do not appear to have been affected by deformation.

PERIOD		GROUP OR FORMATION		LITHOLOGY	THICK-NESS	TRIPOD CODE *
TERTIARY		Porcupine Hills		Interbedded fluvial sandstones and mudstones	?	T
		Willow Creek		Varicoloured siltstones and shales	100 - 835	t
CRETACEOUS	UPPER	St. Mary River		Interbedded fluvial sandstones, carbonaceous shales and coal	500 +	K
		Bearpaw		Dark grey silty shales and sandstones	175	P
		Belly River		Interbedded fluvial sandstones and mudstones with thin coal seams	560 +	B
		Wapiabi		Black to dark grey marine shale with abundant siderite concretions and siltstone interbeds	305	S
		Cardium		Marine sandstones, shales and sideritized chert pebble conglomerates	75 - 80	C
		Blackstone		Dark marine shales with siderite concretions and thin siltstone interbeds	275	W
	LOWER	Blairmore	Beaver Mines	Interbedded ss, green and red shale	275 +	Q
			Gladstone	Interbedded ss, siltst.,shale, congl.		
			Cadomin	Coarse, chert rich ss and congl.		
		Kootenay		Interbedded Sandstone and mudstone with numerous coal seams	35	
JURASSIC		Fernie		Marine shales coarsening upward into interbedded sandstone and mudstone	100	F
MISSISS-IPPIAN		Banff		Competent massive limestones and dolostones	520	M
		Rundle		Shaley mudstones grading upward into massive dolostones		
		Exshaw		Black, platy fissile shale		
Devonian		Wabamun		Interbedded clastics, carbonates and evaporites grading upward into massive interbedded limestones, dolostones and shales.	460	Pa
		Leduc				FH
Cambrian				Marine terriginous clastics interbedded with dolostones and limestones.	?	CS

(* Note: Horizon codes designating contacts for units are accompanied by the subscript 'c', faulted units by the subscript 'f' (ie. Belly River contact = Bc, Belly River faulted = Bf))
All thicknesses are in metres.

Table 1: Table of Formations (Modified from MacKay, 1991).

Mississippian

Mississippian strata have been penetrated by several wells and have an average thickness of 520 m. Shale, siltstone and argillaceous carbonates of the Exshaw and Banff Formations are overlain by platform carbonates and minor terrigenous clastic sediments of the Rundle Group. The Exshaw Formation, consists of thin, black, platy shale with chert nodules and appears to be a major glide horizon (Oswald, 1964; Mackay, 1991). The Rundle Group carbonates behave as a competent structural unit (Mackay, 1991).

Fernie Formation

The Fernie Formation, approximately 100 m thick, consists of brown, dark grey and black, laminated and papery shales. Interbedded dark phosphatic sandstones and limestones and cherty limestones become abundant near the top. A major unconformity separates strata of the Fernie Formation from the underlying Mississippian units. Cruden and Charlesworth (1966) suggest that Mississippian and Jurassic beds near Nordegg, Alberta are separated by a 4° angular unconformity. This angularity was determined from outcrop in more internal portions of the Foothills. Recent workers in adjacent areas to this study (Dwyer, 1986; MacKay, 1991) have not documented any angularity. For this reason, the Fernie Formation and underlying Mississippian units are believed to be parallel in the study area. The top of the Fernie Formation is a major detachment horizon within the study area.

Kootenay Group

The Kootenay Group, approximately 35 m thick, consists of interbedded sandstones, siltstones, shales and coals with minor chert pebble conglomerates.

Blairmore Group

The Blairmore Group, over 275 m thick, disconformably overlies the Kootenay Group. It is the oldest unit to crop out within the study area. It

consists of the Cadomin, Gladstone and Beaver Mines Formations (McLean, 1990A).

The Cadomin Formation is characterized by polymict conglomerate. Other lithologies include conglomeratic sandstone, sandstone, siltstone, mudstone and coal (McLean, 1977).

The Gladstone Formation consists of two informal members. The lower member consists of sandstone and light grey-green to maroon siltstone and shale. The upper member consists of limestone and coquina beds with calcareous mudstone, siltstone and limestone (McLean, 1990b).

The Beaver Mines Formation consists mainly of greenish grey, fine to coarse grained sandstone, with greenish grey and maroon mudstone, siltstone, very fine grained sandstone and minor volcanic beds.

Alberta Group

The Alberta Group is divided into the Blackstone, Cardium and Wapiabi Formations (Stott, 1963).

The Blackstone Formation, approximately 275 m thick, consists mainly of dark grey to black marine mudstone and siltstone with minor beds of argillaceous limestone, sandstone, bentonite and sideritic concretions (Stott, 1990a). The contact with the underlying Blairmore Group is disconformable; the contact with the overlying Cardium Formation is transitional and conformable (Wall and Rosene, 1977).

The Cardium Formation is approximately 75 - 80 m thick, consisting of rubbly, fine grained, marine silty shales and sandstones. Chert pebble conglomerate was identified (Douglas, 1950) close to the southern border of the Langford creek map area and in the southern part of the Callum Creek map area. In well #8 (Figure 2), the formation consist of highly bioturbated, dark grey to black silty shales, with thin (< 1.0 - 4.0 cm), ripple laminated and cross-bedded sands. Rare, thin and discontinuous chert beds and siderite nodules are present (Stott, 1963; Wall and Rosene, 1977).

The Wapiabi Formation, approximately 305 m thick, consists of thinly bedded, dark grey, marine shales. Some parts contain abundant siderite concretions, minor siltstone, sandstone and limestone. The formation grades upward into interbedded marine mudstones and sandstones (Stott, 1990b; Douglas, 1950).

Belly River Formation

The Belly River Formation is the sequence of fluvio-deltaic sediments which are sharply, but conformably overlain by the Bearpaw Formation and conformably overlie the Wapiabi Formation. The formation is a prominent ridge forming unit. Its average thickness in wells within the study area is approximately 560 m, but it likely thickens to the west. The lowest unit is 30-50 m. thick and consists of dark grey, thinly bedded, fine grained, dark brown weathering sandstones. These strata are transitional to the underlying Wapiabi Formation. Approximately 168 m of very massive, thick, coarse, light grey, cross-bedded sandstone with minor amounts of grey and green shale overlie the transition beds. Overlying these strata are interbedded, fine to medium grained, cross-bedded, grey to green sandstone and grey and green, silty shales. The upper 250-275 m consists of pale green weathering, green and grey shales, thin-bedded, fine grained, grey sandstones, rubbly concretionary argillaceous limestones and minor carbonaceous shale and coal seams (Douglas, 1950; Wall and Rosene, 1977; Nelson and Glaister, 1983).

Bearpaw Formation

The Bearpaw Formation consists of dark grey, carbonaceous, thin bedded silty shales and interbedded sandstones (Douglas, 1950; Caldwell, 1990). The shales are silty, carbonaceous and light grey-brown in well #8 (Figure 2). They are darker and less silty in well #5 (Figure 2). The contacts with the overlying St. Mary River Formation and underlying Belly River Formation are conformable and gradational, making it difficult to pick formation tops from cuttings and

geophysical logs. The base and top of the formation were picked from drill cuttings at the positions where significant coal occurs, or where green-grey shales and grey sandstones predominate over silty carbonaceous shales. The stratigraphic thickness, 175 m in well #10 situated close to the axial plane of the Alberta syncline, decreases both to the west and north. Where present, the Bearpaw Formation has been structurally thickened in all other wells, the farther west the well the greater the amount of thickening. In well #5 (Figure 2), the Bearpaw Formation is two to three times the normal thickness. Well #10 (Figure 2) is the farthest to the east and likely encountered the closest approximation to true stratigraphic thickness.

St. Mary River Formation

The St. Mary River Formation, approximately 500 - 550 m. thick, consists of lower and upper parts (Wall and Russel, 1990). The lower part consists of coarse to medium grained, reddish brown weathering, grey sandstones, dark grey, green and carbonaceous shale, coal seams, thin ironstone bands, and oyster coquinas. The upper part of the formation is composed of a series of interbedded lenticular sandstones, shales and freshwater limestones or ironstones. The shales are olive green, grey, carbonaceous, silty, and calcareous. The 'ironstones' are massive beds, 0.3 to 1 m thick and grade laterally into sandstones or shales or form caps on underlying sandstones. Both the upper contact with the Willow Creek Formation and the basal contact with the Bearpaw Formation are conformable and gradational. With the exception of the transitional basal portion, the strata are non-marine (Wall and Rosene, 1977). The St Mary River Formation grades into the Edmonton Formation to the north (Zaitlin, 1983).

Willow Creek Formation

The Willow Creek Formation consists of varicoloured shales with calcareous concretions and soft, light grey sandstones (Wall et al., 1990). The formation thins, from over 835 m in the south to less than 550 m in north, and

decreases to zero in the southern part of the Stimson Creek map area (Hume, 1940). The contacts of the Willow Creek Formation were very difficult to pick from geophysical logs and chip samples. They were picked where varicoloured shales of the formation were less abundant in chip samples than the sandstones of the overlying and underlying units.

Porcupine Hills Formation

The Porcupine Hills Formation is Tertiary in age and composed of olive brown shales interbedded with fine to coarse grained brownish grey, cross-bedded limy sandstone and calcareous siltstone (Turner, 1990). The top of the formation was not encountered within the study area, so its thickness is unknown.

Thickness determination

The thicknesses cited above for the Blairmore Group (275 + m), the Belly River Formation (560 + m) and the St. Mary River Formation (500-550 m), are substantially less than those determined by Douglas (1950), namely 305-670 m, 914-1280 m, and 971 m, respectively. The reasons for this discrepancy are uncertain. All of the averaged thicknesses for these units were derived from thicknesses encountered in wells in relatively undeformed strata toward the eastern part of the thesis area. Most of Douglas' thicknesses were derived from outcrops in the western part of the study area. All three units contain coarse clastics and likely thicken substantially to the west. The thicknesses used in this study may, therefore, represent minimum thicknesses for these units. Alternatively, the thicknesses of Douglas (1950), estimated from poorly exposed outcrop sections within the foothills belt where substantial structural thickening may have occurred, may be in error.

CHAPTER 3
STRUCTURAL GEOLOGY AND SETTING

The structure of the Canadian Rocky Mountain Fold and Thrust Belt is dominated by thrust faults, almost all of which are east verging. Mechanical anisotropy due to stratigraphic layering exerts a profound influence on deformation styles. Strata are dominated by flexural slip folds related to the geometry of underlying fault surfaces (Price, 1981). Three main types of fold occur (Figure 3): fault-bend, fault-propagation and detachment folds (Suppe, 1983; Mitra and Namson, 1990). Fault bend and fault propagation folds appear to dominate the structure of the Langford Creek region. Thrust faults cut up section along ramps that link bedding plane glide horizons. Fault-bend folds form at the intersection of fault ramps and flats. Movement along younger thrusts at deeper structural levels has deformed all overlying thrust sheets. This phenomenon was first documented in the Canadian Rockies by Hake et al. (1942) and Douglas (1950). A less recognized, but potentially very important deformation mechanism is layer parallel shortening (Figure 3d). Layer parallel shortening is accomplished by the development of solution cleavage, microscopic and mesoscopic folding, plastic deformation and other effects (Hatcher et al., 1989). Deformation associated with layer parallel shortening will be discussed in more detail in Chapter 7.

Axial culminations and depressions have long been recognized in the Canadian Rocky Mountains and other fold and thrust belts. Bally et al. (1966) suggested that these features may be related to three factors: 1) basement highs or structural involvement of basement at depth, 2) stacked imbrications at depth or 3) variations in thickness of the stratigraphic sequence involved in the thrust sheet. Seismic and drillhole evidence has convincingly eliminated the possibility of basement involvement in most of the Canadian Rocky Mountains. Axial culminations and depressions are likely related to stacked imbrications, variations in the thickness of the stratigraphic sequence involved in a thrust sheet, or a

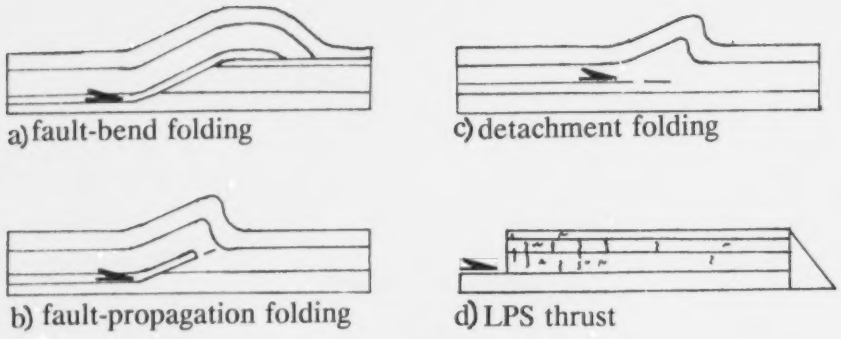

Figure 3: a-c) Three main types of fold-thrust relationships encountered in the Rocky Mountains (modified from Jamison, 1987). d) Thrusting with layer parallel shortening; shortening is accomplished by development of solution cleavage, mesoscopic deformation, pressure solution assisted grain boundary sliding and other effects (modified from Hatcher et al, 1989).

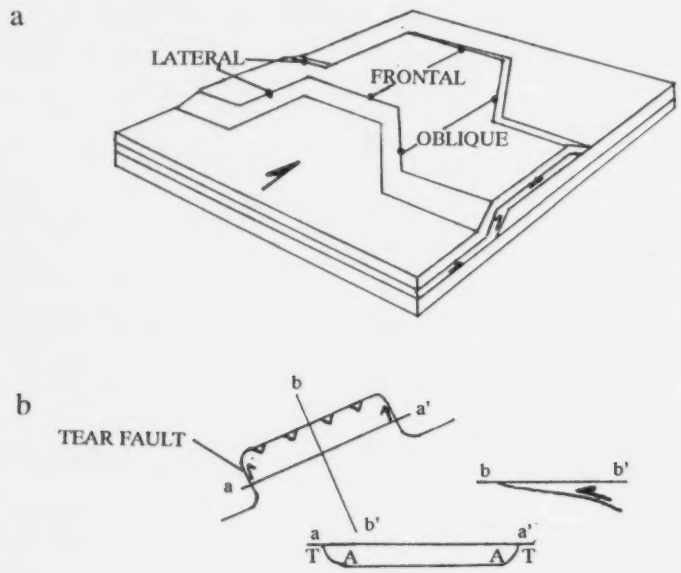

Figure 4: a) Block diagram of lateral, oblique and frontal ramps and related folds. Lateral and oblique ramp anticlines are formed by the translation a thrust sheet over lateral and oblique ramps, respectively. These structures result in structural culminations and depressions in Foreland Fold and Thrust belts (modified from McClay, 1992). b) Tear fault; displacement along the thrust fault terminates abruptly at strike-slip faults (modified from Hatcher, 1990).

combination of both. Variations in the thickness of strata in a thrust sheet result from the existence of lateral ramps. A lateral ramp is defined as a ramp in the thrust surface that is parallel to the direction of transport of the thrust sheet (McClay, 1992). A tear fault is a strike-slip fault which ends downward against a detachment and, while active, intersects the topographic surface (Figure 4). Dahlstrom (1970) elegantly explained the genesis of axial culminations and depressions with their relationship to lateral ramps. His definitions of tear faults and lateral ramps are not clear, however, and the definition of McClay (1992) is preferred.

The southern Canadian Rocky Mountains are commonly bounded at the foreland leading edge by an east dipping thrust. Predominantly east verging thrusts have wedged strata beneath the east dipping thrust or have transported these strata toward the foreland along bedding plane glide zones (Jones, 1982; Charlesworth and Gagnon, 1985). The wedging of strata forms a volume of complex, internally deformed strata which has a roughly triangular shape (Figure 5), commonly called the triangle zone or delta structure (Gordy et al., 1977; MacKay, 1991). Early interpretations (Figures 6a and 6b) of the triangle zone at Turner Valley, approximately 60 km north of the Chain Lakes Reservoir, were largely in error due to the prevailing belief that the east verging thrusts cut up section to the surface (Clark, 1954; Bossart, 1957). The resulting structure sections were often unrealistic and surface thrusts had to be 'invented' to account for the significant displacement at depth. Later workers (Gordy et al, 1977; Jones, 1982; Mackay, 1991) showed the structure as resulting from east verging blind thrusts flattening along bedding plane glide zones and wedging strata beneath an east dipping detachment zone.

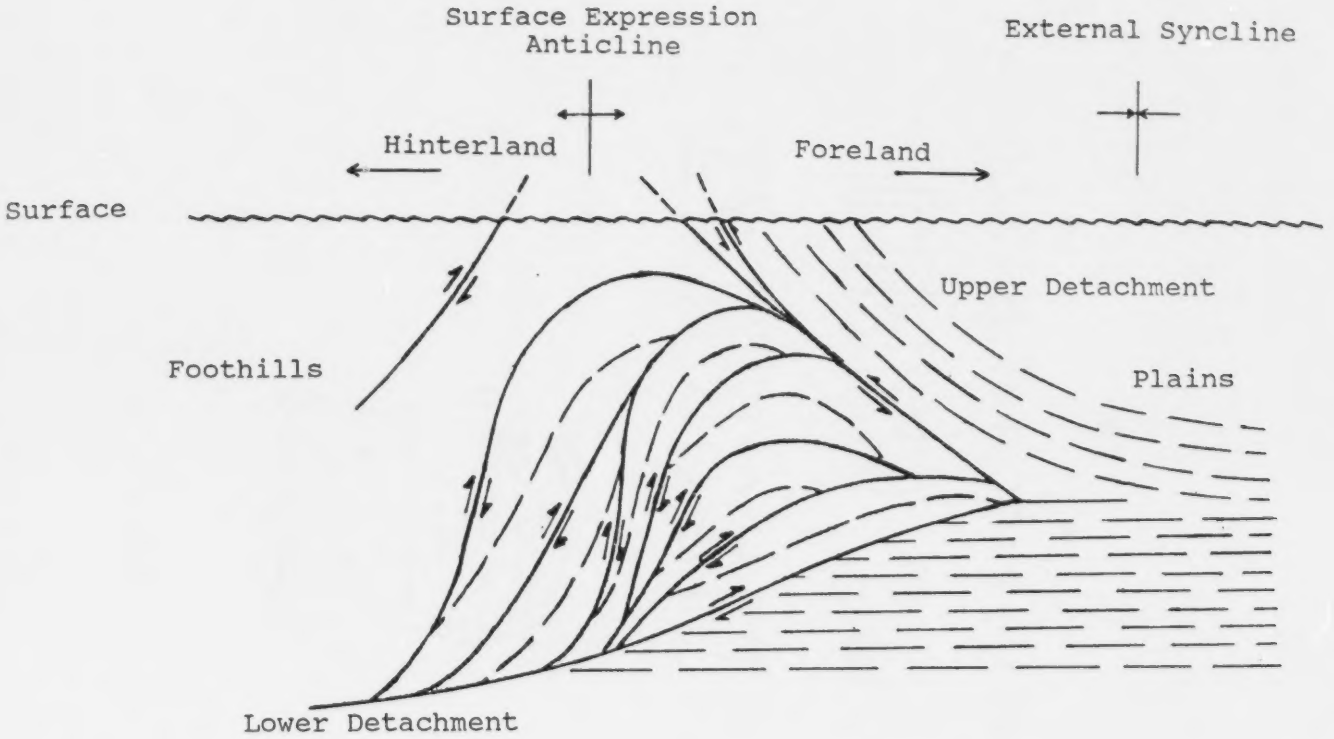

Figure 5: Idealized Triangle Zone - Hinterland dipping, foreland verging thrusts are wedged below the foreland dipping upper detachment surface. The lower detachment surface ramps to a higher stratigraphic level, transporting the wedge toward the foreland (Modified from MacKay, 1991).

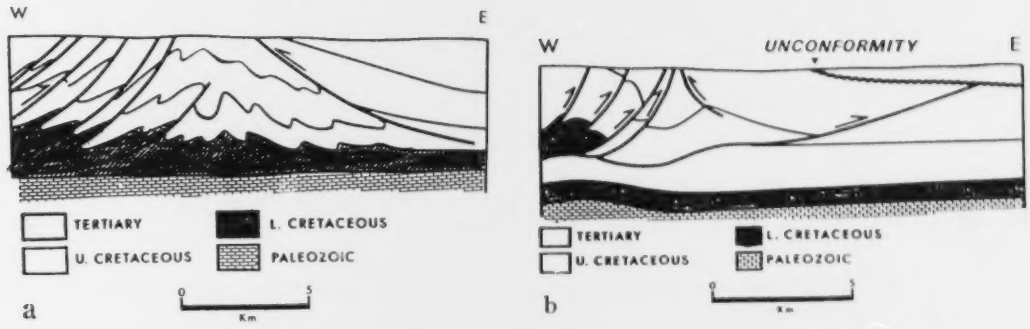

Figure 6: Early interpretations of the structure of the triangle zone. a) Most foreland verging thrusts propagate to the surface; the geometry beneath the hinterland verging backthrust is very uncertain (After Clark, 1954). b) A post thrusting unconformity is invoked to explain the absence of thrusts cropping out beyond the west flank of the Alberta Syncline. Problems result from this model when the overlying unconformity must be tilted without affecting the underlying units (After Bossart, 1957). Both diagrams modified from Jones (1982).

CHAPTER 4
DATA COLLECTION, ANALYSIS AND STORAGE

Collection and storage of outcrop and drillhole data

Outcrop and drillhole data were digitized and placed in ASCII computer data files (see Appendix 1 for format). Universal Transverse Mercator Grid coordinates were used to record positions (in metres). These data were digitized using a Summagraphics Model ID-2-TAB-3040 digitizing tablet, attached to a Zenith Datasystems 386/25 personal computer. An interactive digitizing program, EZDIGIT Version 1.01 (Guidos, 1991) was used to digitize most of the surface and subsurface data.

Outcrop data

Much of the outcrop information was digitized from four Geological Survey of Canada (G.S.C.) 1:63 360 map sheets: the Gap 978A, Callum Creek 982A, Langford Creek 981A (Douglas, 1949A, 1949B, 1949C) and Livingstone River preliminary map sheet 5-1958 (Norris, 1958). Additional outcrop data, acquired by the author during September, 1991 were digitized using NTS 1:50 000 map sheets 82J/1 and 82G/16.

The original G.S.C. maps were plotted on Township and Range grids displaying lines of latitude and longitude. In order to digitize the geologic data, a Universal Transverse Mercator (UTM) grid was transferred manually onto the G.S.C. maps. The coordinates of selected UTM grid points were measured relative to the lines of longitude and latitude on the NTS map sheets. A scale factor was used to recalculate and plot these coordinates relative to the latitude and longitude lines on the G.S.C. maps (Figure 7):

Scale Factor = 50000/63360 = 0.7891414

The relative positions of these lines were visually checked with respect to topographic and other features plotted on both maps. An additional check was provided by digitizing several points on the G.S.C. maps and comparing the coordinates with the UTM grid on NTS maps.

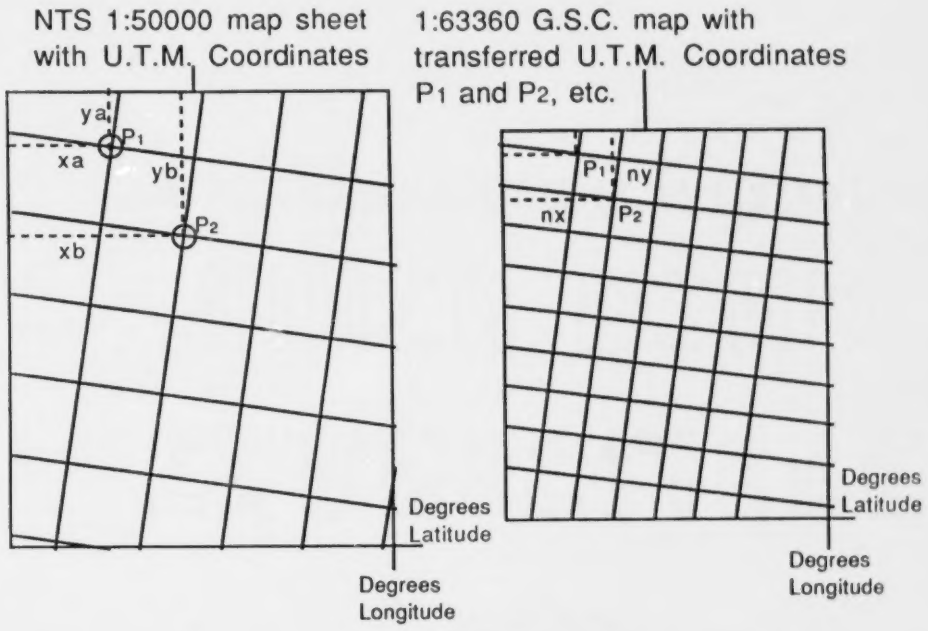

Figure 7: Selected UTM points (P_1, P_2) on the 1:50000 contour maps are measured relative to lines of latitude and longitude. These values (xa, ya, xb, yb) are multiplied by the Scale Factor (0.7891414) to give the appropriate distance on the 1:63360 map (xa * 0.7891414 = nx; xb * 0.7891414 = ny).

Outcrop data recorded were placed in ASCII files (Appendix 1) and consisted of UTM coordinates, elevation, a code specifying the stratigraphic unit to which the exposed strata belong, and various orientation measurements (dip direction, dip, plunge of minor folds, pitch etc.). Elevations were recorded in feet and converted to metres.

Field data were obtained by the author during September, 1991. Field locations were recorded on 1:50 000 NTS map sheets, with a location number corresponding to an appropriate entry in a field note book. Orientation measurements, lithology, elevation and other observations were recorded in the

field note book. The orientations of bedding and other mesoscopic structures were recorded using a Silva compass. Field locations were digitized using the UTM grid on the NTS maps and placed in ASCII data files.

Maps, at 1:50 000 and 1: 63 360 scales, displaying the positions of outcrops, horizon code, elevation and orientation of outcrop data were constructed as discussed below. These maps were compared with G.S.C. maps and UTM coordinates. Wrongly positioned outcrops were redigitized or deleted. Various kinds of error were introduced while digitizing the data. One of the most obvious results from transferring the NTS grid to the G.S.C. maps. These errors were kept to a minimum by recalculating and calibrating the grid. All G.S.C. maps had been folded and it was difficult to keep these maps completely flat while digitizing points, thereby introducing one source of error. Errors associated with paper stretch are also difficult to avoid. Locations often had to be redigitized using smaller UTM grid intervals to minimize these errors. Some field stations using NTS maps were difficult to locate precisely, resulting in error. Errors of 50 m up to 100 m horizontally and 50 m vertically may be present. Several measurements of bedding were taken where exposure permitted in order to minimize errors associated with irregularities, small scale structures and instrument or measurement inaccuracies. Cumulative errors in the horizontal position of outcrop data are probably less than 100 m. The NTS maps reveal errors in the topographic base map used by the G.S.C.. For example, the elevation of Mt. Livingstone on map 5-1958 is recorded as 2435.8 m and 2421.2 m on NTS maps 82J/1, a difference of 14.6 m). The magnitude of these errors is considered insignificant for the purposes of this study (15 m corresponds to 3 mm on 1:50,000 scale plots used for cross sections).

Drillhole data

Drillhole data were digitized and placed in ASCII files. The drillhole data used in this study included dipmeter, deviation and stratigraphic information. The format of the ASCII data records is shown in Appendix 1. Kelly Bushing

coordinates were digitized from a 1:50 000 base map. Stratigraphic data and fault contacts were picked using geophysical logs, lithology logs and dipmeter data. Gamma ray - sonic logs were utilized in most wells to make these picks; in some of the older wells acoustic logs were not run or were of poor quality. In these wells, electric, neutron, density or lithology logs were used. Deviation data for two wells, 2-29-13-2W5 and 15-15-12-2W5, were supplied by Husky Resources in the form of digitized ASCII data files. These data were combined to form the drillhole raw data file.

Dipmeter data were supplied by Husky Resources for three wells: 2-29-13-2W5, 15-15-12-2W5 and 16-29-14-2W5. Data for well 2-29 were supplied in the form of a paper log with dipmeter readings averaged over varying intervals. The readings were cited as dip direction and dip and were entered into the drillhole data file. The quality of dipmeter readings in Well 2-29, drilled in 1956, is poor. Fortunately this well was extensively cored. Core-bedding angles were measured for selected cores throughout the well and used to check the dipmeter readings. Plots of the deviated drillhole and dipmeter readings were constructed as discussed below.

Dipmeter data for wells 15-15-12-2W5 and 16-29-14-2W5 were supplied in the form of paper logs with standard tadpole plots displaying dip direction, dip and quality of the dipmeter correlations. Only high quality readings were digitized. Readings displaying a high degree of scatter, inconsistent dip direction or dip were ignored. Dipmeter readings are of higher quality in shalier intervals, with cross bedded sandstones and carbonates displaying higher degrees of scatter. ASCII files containing digitized dipmeter data were imported to the spreadsheet program QUATTRO PRO, sorted by depth and converted from feet to metres if necessary.

Analysis of outcrop and drillhole data

Outcrop analysis and domain specification

The raw outcrop data files were imported into the computer program TRIPOD (Charlesworth et al., 1989) to form the database CHAIN. TRIPOD is a microcomputer program developed at the University of Alberta for storing, retrieving, displaying and analysing orientation, stratigraphic and positional data from drillholes, outcrops and seismic lines. TRIPOD was used to perform various statistical analyses of these data. Outcrops were grouped into 10 domains within which strata could be considered to be either cylindrically folded or appeared to have a uniform orientation (Figure 8). Provisional boundaries for these domains were chosen using the traces of faults and modified later, if necessary. Several tests to determine the cylindricity of folding were carried out by the program; the different tests have been discussed in detail by Charlesworth et al. (1989). If folding is cylindrical, TRIPOD returns the value of the fold axis for each domain. Orientation diagrams (Appendix 2) were constructed for each domain. Outcrops and drillholes within these domains were projected axially onto planes of cross section.

Orientation diagrams constructed for domains 1, 6 and 7 show that strata within these domains have relatively uniform orientations. The mean orientation for strata within these domains was calculated from the eigenvector associated with the maximum eigenvalue of the orientation matrix (Charlesworth et al. 1976). Outcrop and drillhole data were projected horizontally, parallel to the strike of the mean orientation, onto the plane of cross section. The results of the domain tests, outcrop analyses and the projection direction within each domain are summarized on Table 2.

Dipmeter analysis

The ASCII data files containing dipmeter data were used to create Statistical Curvature Analysis Technique (SCAT) (Bengston, 1981, 1982) plots

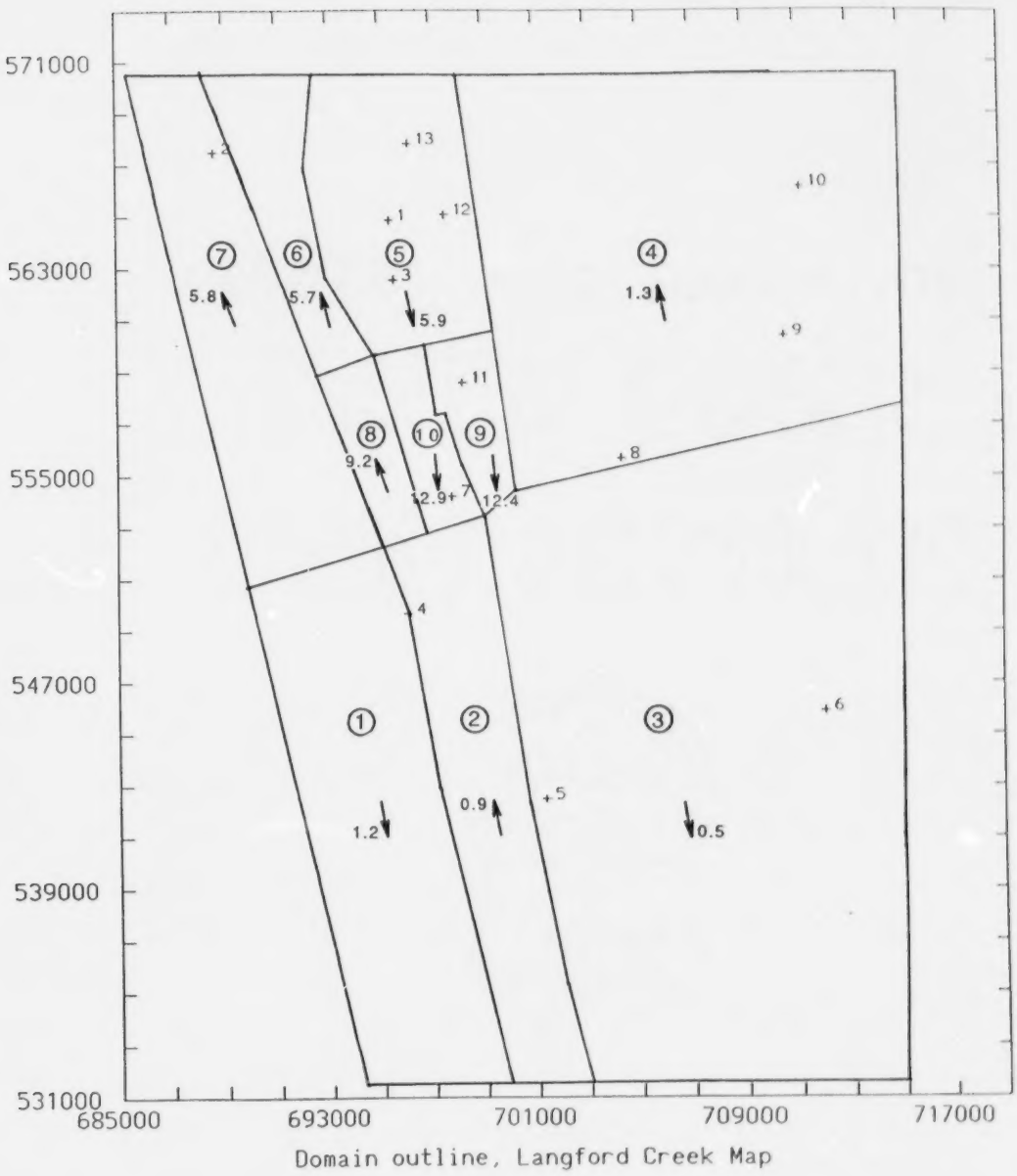

Figure 8: Map of domain boundaries within the Langford Creek study area. Arrows indicate trend and plunge of fold axes within each domain.

Domain #	Eigen Vectors (Trend Plunge)	Eig. Values Eval/N	Projection Dir. (Trend Plunge)	Cylindricity Index (6 tests)
Entire Map Area	E1: 275.5 85.4 E2: 79.1 4.5 E3: 169.2 1.1	0.50 0.45 0.02	169.2 1.1	not tested
1	E1: 80.1 28.1 E2: 263.1 61.8 E3: 170.7 1.2	0.91 0.08 0.01	170.1 0	Cluster
2	E1: 80.2 37.2 E2: 258.4 52.8 E3: 349.5 0.9	0.80 0.19 0.01	349.5 0.9	4 of 6
3	E1: 259.6 61.0 E2: 78.3 29.0 E3: 168.6 0.5	0.89 0.10 0.01	168.6 0.5	5 of 6
4	E1: 257.5 66.5 E2: 81.0 23.5 E3: 350.4 1.3	0.88 0.11 0.00	350.4 1.3	4 of 6
5	E1: 78.3 20.9 E2: 275.5 68.2 E3: 170.6 5.9	0.65 0.33 0.01	170.6 5.9	3 of 5
6	E1: 80.4 27.3 E2: 246.5 62.0 E3: 347.4 5.7	0.84 0.12 0.04	170.4 0	Cluster
7	E1: 71.8 41.5 E2: 240.1 47.9 E3: 336.6 5.8	0.84 0.13 0.03	161.8 0	Cluster
8	E1: 78.3 47.6 E2: 240.0 40.9 E3: 338.1 9.2	0.81 0.18 0.02	338.1 9.2	3 of 6
9	E1: 337.0 77.1 E2: 82.3 3.5 E3: 173.1 12.4	0.50 0.48 0.02	173.1 12.4	4 of 6
10	E1: 75.3 37.1 E2: 281.1 50.0 E3: 175.3 12.9	0.71 0.24 0.05	175.3 12.9	3 of 6

Table 2: Summary of domain analyses and resulting projection directions used to construct geologic cross sections.

using the computer program SCAT, a software package developed by the University of Alberta structural geology group. The computer program Orient (Charlesworth and Jahans, 1991) was used to construct orientation diagrams of dipmeter data. SCAT plots display the azimuth, dip and depth components of the dipmeter data in various formats (Appendix 3). They are used to delineate faults, stratigraphic contacts, areas of plunge, fold shape and axial surfaces of folds (Bengston, ibid.). The data derived from SCAT plots and orientation diagrams assisted the construction of the balanced cross sections. SCAT plots were generated for all wells (Appendix 3). Dipmeter data from well 15-15 are very informative, fault contacts and plunging folds being immediately apparent from the various plots. Well 16-29-14-2W5 dipmeter readings display a high degree of

scatter throughout. Most of the dipmeter readings for this well were recorded in shallow dipping coarse clastic strata. Accurate dipmeter determination of azimuth of dip for shallow dipping to horizontal beds is difficult. The random distribution of azimuth of dip for these data is likely due to the limitations of the dipmeter for shallow dipping beds. The high degree of scatter is also due to stratigraphic effects such as cross bedding, and possibly other mesoscopic structures. Dipmeter correlations are more reliable for shallow to moderate dipping beds, as a result, statistical analyses tend to be biased toward shallower dips. The magnitude of this bias is difficult to determine and varies from well to well. SCAT plots for well 2-29 did not provide any useful information due to the low number of readings and are not included in Appendix 3.

TRIPOD can also be used to process and display dipmeter data. Before the dipmeter readings for well 16-25 and 15-15 could be imported into the database WELLS, the number of readings in the raw ASCII files had to be reduced. A computer program PENDNQ (Charlesworth, 1992) was used to do this. PENDNQ averages the data over a specified interval. The program can also be used to eliminate averaged readings with a high degree of dispersion.

CHAPTER 5
SEISMIC DATA

Seismic processing and interpretation

Five seismic sections were supplied by Husky Resources Limited (Figure 9). Access was also provided to data from three proprietary seismic lines. Tracings of these lines were made to assist structural interpretation. All seismic sections are unmigrated, 24-fold (2400%), air shot, dynamite source data.

The seismic sections were used in the construction of the balanced and partially balanced geologic cross sections. In order to interpret the seismic data accurately, two way travel time must be converted to depth. Seismic measurements give estimates of the subsurface geometry and acoustic impedance of the rocks (Neidell, 1979). Stratigraphic and structural correlation of seismic data was accomplished using synthetic seismograms that were supplied by Husky Resources.

The percentage of seismic energy reflected at an interface depends on the acoustic impedances of the materials on respective sides of an interface and the angle of incidence of the down-going wave. Spherical wavefronts with large radii may be treated as planes. Using this assumption, lines perpendicular to wavefronts (wave paths or rays) may be used to describe the wave propagation. At normal incidence, the amplitude of a reflection depends on the acoustic impedances across a boundary. The energy of a reflected compressional wave remains almost constant with increasing angle of incidence until the critical angle is approached. As this angle is approached, an increasing amount of compressional wave energy is converted to refracted and reflected shear energy. For a horizontal reflecting surface, the depth (z) of a reflector in a constant velocity layer is given by the following formula:

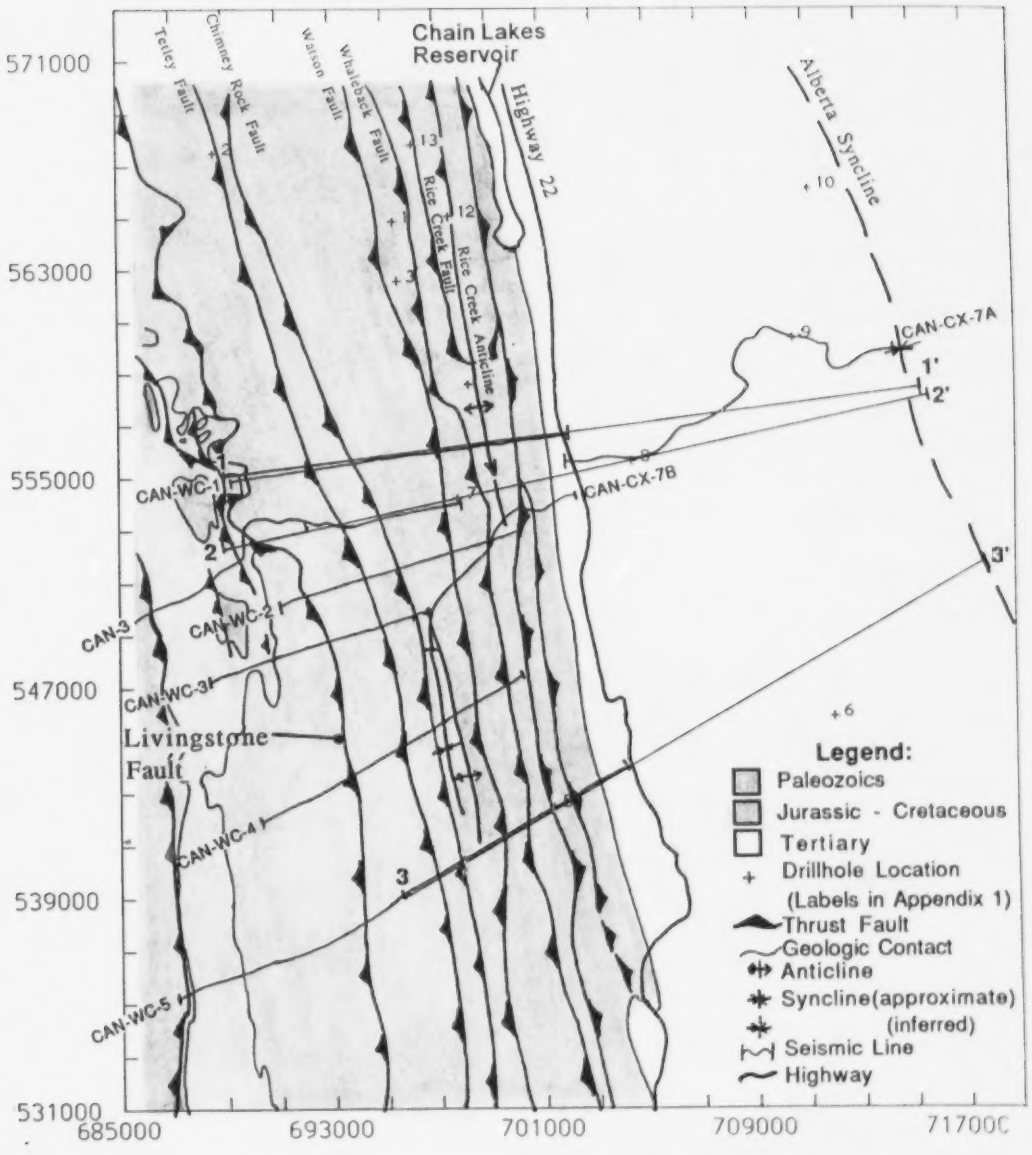

Figure 9: Map showing positions of seismic lines used in this study, geology modified after Douglas (1950). The locations of 3 balanced cross sections

$$z = \frac{\sqrt{(V_1 T)^2 - x^2}}{2}$$

where x is the distance between the shot and the reflector, T is the total travel time for a reflected wave and V_1 the seismic velocity above the reflecting surface (Figure 10). These assumptions form the basis of the seismic reflection method (Dobrin and Savit, 1988).

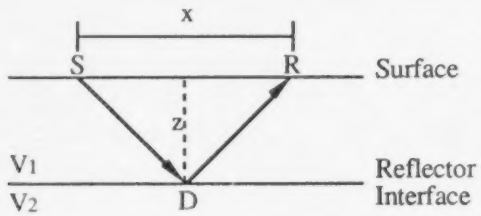

Figure 10: Wave reflected from a horizontal interface, with constant velocity (V_1) between the source and interface. Modified from Dobrin and Savit (1988).

Synthetic seismograms are the basic tool for integrating geologic and seismic data. The construction of synthetic seismograms, first discussed by Peterson et al. (1955) and Wuenschel (1960), is based on the assumption that a laterally restricted segment of the earth around a borehole can be taken as a horizontal layered medium. A plane wave is assumed to propagate in this medium, and the seismogram is made up of partial reflections of the plane wave from each of the planar boundaries (eg. lithologic contacts). The velocity and density of different lithologies are not equal, these factors affect the reflection and transmission coefficients at a lithologic boundary.

The product of the velocity and density of a material is known as the acoustic impedance. The reflection coefficient and the transmission coefficient which characterize the amplitudes of the reflected and transmitted waves can be written in terms of the acoustic impedance (Neidell, 1979). The reflection coefficient (r) and the transmission coefficient (t) may be written as follows:

$$r = \frac{D_1}{A_1} = \frac{\delta_2 V_2 - \delta_1 V_1}{\delta_2 V_2 + \delta_1 V_1}; \quad t = \frac{A_2}{A_1} = \frac{2\delta_1 V_1}{\delta_2 V_2 + \delta_1 V_1}$$

Where δ_1, δ_2 are the densities (Mg/m^3) of the media, V_1, V_2 are the internal velocities (m/s), A_i is the amplitude of the incident wave, D_i is the amplitude of the reflected plane wave, and A_2 is the amplitude of the transmitted plane wave. The acoustic impedance ($V * \delta$) decreases with depth. Density contrasts on opposite sides of lithologic contacts are usually small. As a result, the acoustic impedance depends mainly on the velocity contrast across the contact (Neidell, 1979).

To construct a synthetic wavelet, formation tops must be 'picked' from gamma ray - sonic or other geophysical logs and average interval velocities are calculated for specific formations or groups of formations from travel times on digitized acoustic logs. The drillhole can then be blocked into intervals of constant velocity and the corresponding plots of acoustic impedance, reflection coefficient and the synthetic seismogram can be constructed and correlated with seismic sections

Synthetic seismograms suggest that the Cambrian, Mississippian and the Kootenay-Fernie Intervals are good reflectors. These horizons correlate well on seismic sections. Moderate, poor or discontinuous reflectors occur within the Blairmore, Cardium, basal Belly River and the Bearpaw Formations. Once preliminary identification of seismic reflectors has been made, comparison between adjacent seismic lines is conducted.

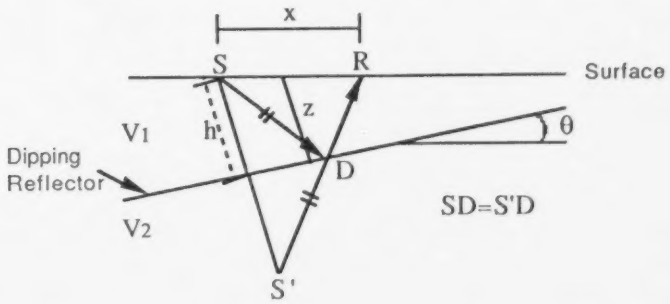

Figure 11: Ray path trajectories and time-distance relationships for a dipping bed.

A common-depth-point stacked seismic section shows reflections in vertical positions that correspond to vertical travel paths. If reflectors are dipping or irregular, the position and attitude of reflectors are distorted. For a reflecting surface dipping at an angle θ (Figure 11), the velocities of the materials above and below the reflector are V_1 and V_2 respectively, S is the position of the source and R the receiver. Reflected waves recorded at R can be considered as waves from S' which is the mirror image of S with respect to the reflector. T is the total travel time for the ray path SDR, x is the horizontal distance between S and R. From the law of cosines, we can write:

$$(V_1T)^2 = (2h)^2 + x^2 - 2(2h)^2 x\cos(\frac{\pi}{2}-\theta)$$
$$= 4h^2 + x^2 - 4hx\ \sin\theta$$

on all exploration seismic sections, $x^2 << 4h^2$, therefore

$$V_1^2T \approx 4h^2 - 4hx\ \sin\theta$$

for a zero offset source-receiver pair, $V_1T = 2z$

$$(2z)^2 = 4h^2 - 4hx\ \sin\theta$$

differentiating with respect to x, we obtain

$$4z\ \frac{dz}{dx} = -4h\ \sin\theta$$

if h = z (zero-offset case)

$$-\sin\theta = \frac{dz}{dx}; \qquad \tan\beta = \sin\theta$$

where ß is the apparent dip and θ is the true dip of the reflector.

Migration is a process which attempts to reposition reflectors recorded in two way travel time, in order to make them more closely resemble the geometry of structures at depth (McQuillan et al., 1984). Several methods of migration,

both manual and mechanical, have been developed over the past 50 years. Figure 12 shows wrongly positioned dipping reflector. Reflections R1 and R2 on a reflector of slope ϴ are recorded at the zero-offset source-receiver pairs A and B. These reflector points are plotted as R1' and R2' along vertical lines below A and B. These points define an incorrectly positioned reflector of slope ß. From this diagram:

$$(1)\quad \tan\beta = \sin\Theta,$$
$$(2)\quad \sin\Theta = V_1 \frac{dt}{dx}$$

equation (1) may be used to calculate the correct dip of an unmigrated reflector. For shallow dips (5° - 15°), tan ß ≈ sin ß, at steeper dips this relationship breaks down (a 45° apparent dip equals a 90° corrected dip). Significant error (> 10%) results from apparent dips steeper than 25°. The position of these reflectors will also be significantly in error. Equation (2) may be used to correct these errors, but this was not done due to uncertainty about the proper values of velocity to use in migration. Seismic dips steeper than 25° are poorly imaged on the seismic sections. The position and true dip for steeply dipping reflectors are corrected using outcrop and drillhole data or the kink-fold method discussed later. Detailed discussions of the various migration methods are provided by Hood (1981); McQuillan et al. (1984) and Robinson (1983). On unmigrated seismic sections structures are distorted or masked; synclines are tighter, anticlines more open and the positions of axial planes, faults and dipping strata are shifted.

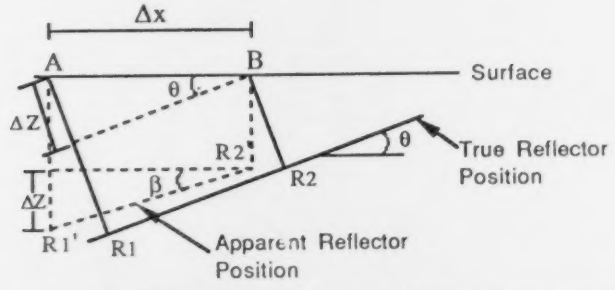

Figure 12: Geometrical relationships used to determine the correct position and dip (ϴ) of and apparent reflector with a dip of ß. Modified from Robinson and Coruh (1988).

Time pullups occur where high velocity strata have been repeated. Mississippian carbonates have a much higher interval velocity (>6000 m/s) than Mesozoic clastics (<3500 - 4500 m/s). In the Langford Creek area, where Mississippian strata have been repeated or thrust over Mesozoic strata, the faster transit time through the Mississippian section decreases the two way travel time to underlying strata, resulting in an apparent pullup on seismic sections. Pullups are very useful on seismic sections for determining the approximate positions of footwall ramps and hangingwall cutoffs for faults which repeat high velocity strata.

CHAPTER 6
MAP AND CROSS SECTION CONSTRUCTION

Geologic maps

Maps displaying the position, elevation, stratigraphic horizon and bedding orientation of outcrops were generated using TRIPOD. Maps were generated to test the accuracy of digitized data, and to assist the construction of cross sections and interpret surface and subsurface geology.

Cross sections

Cross sections 1 and 3 were constructed to coincide with the seismic sections. The position of the cross sections is shown on Figure 9. Cross section 2 passes through drillholes 2-29-13-2W5 and 16-25-12-2W5. The cross sections, which display projected outcrops and drillholes, were constructed at a scale of 1:50 000. Outcrop data more than 500 m from the cross section were not used, whereas the maximum projection distance for drillholes was 3.5 km. Drillholes 1-4-14-2W5, 2-29-13-2W5, 16-25-13-2W5 and 15-15-12-1W5 were projected parallel to the projection direction determined from outcrop and dipmeter analyses. Several thrust sheets may be encountered within a single drillhole. The orientation of fold axes within adjacent thrust sheets commonly varies. Errors may result from the projection of drillholes parallel to a single projection direction. These errors are insignificant where wells are projected short distances (less than 100 m for wells 15-15-12-1W5, 2-29-13-2W5, and 16-25-13-2W5) but may result in significant error if wells are projected longer distances (approximately 3 km for well 1-4-14-2W5).

Regional dip for the top of the Mississippian (257° 2.5°) was determined from downhole coordinates in wells 2-29-13-2W5, 10-10-14-1W5 and 12-26-12-1W5. Wells 10-10 and 12-26 were projected parallel to the strike of the top of the Mississippian onto cross sections to establish the position of autochthonous units on cross sections.

Seismic reflectors were transferred manually onto cross sections by multiplying vertical two-way travel time by an average interval velocity. As mentioned previously (Chapter 5), seismic reflectors on unmigrated seismic sections will be incorrectly positioned. The position of these reflectors may be corrected using the equation $\sin \theta = V\ dt/dx$; this requires accurate velocity data which was not available for this study. The positions of these reflectors were not corrected for this reason. Outcrop and drillhole data were used to correct the attitude and position of many of these reflectors. The kink fold method (Suppe, 1983) was used to interpret the subsurface geology and generate balanced cross sections. Woodward et al. (1983) outline a series of steps, derived from the kink fold method of Suppe and Chang (1983) and Suppe (1983), which assist in the geological interpretation of unmigrated seismic data. The kink fold method involves the following steps:

1) locate regions of homogeneous dip,
2) locate axial surfaces between regions of homogeneous dip,
3) locate major discontinuities in structure where the axial surfaces terminate or branch, and
4) interpret terminations of axial surfaces in terms of fault trajectories.

The kink fold method provides a predictive mathematical model which relates axial surfaces and fold geometry to the trajectories of underlying fault surfaces. An example of the kink fold method is illustrated on Figure 23. A footwall ramp angle of 15° was determined for the Rocking P fault on the bottom left hand side of seismic section WC1, a fore-limb dip of 16° is determined by Suppe (1983). Axial planes are positioned between regions of homogeneous dip. For ramp angles greater than 20° - 25°, small changes in this angle leads to large changes (>10%) in the fore-limb dip determined by Suppe (1983). The average ramp angle for most faults was 15° - 20° with a maximum of approximately 25°. As a result, the kink fold method should give accurate estimations of the fore-limb dip

for most faults. The kink fold method can be used to correct or clarify distorted seismic data and extrapolate these data into areas where no seismic or well data are available (Woodward et al., 1983). All stratigraphic units were line length balanced except for the Bearpaw Formation which was area balanced.

CHAPTER 7
STRUCTURE

Introduction

Three 1:50 000 scale balanced structural cross sections, Sections 1, 2 and 3, have been constructed through the Langford Creek study area. The sections were completed using outcrop, drillhole and seismic data. The location of these sections is shown on Figure 13. All three sections display a prominent zone of disharmony in the Bearpaw Formation. Above the Bearpaw, younger units lie in the west limb of the Alberta Syncline whose dip progressively decreases towards the east. Below this zone, Mississippian to Belly River strata have been displaced toward the foreland by a series of thrusts that flatten in the Bearpaw. Clearly, the zone of disharmony coincides with a major glide zone that will be referred to as the upper detachment. The Bearpaw Formation itself displays considerable intraformational deformation and has everywhere been tectonically thickened.

Mississippian to Belly River structure

Section 1

Strata on cross section 1 (Figure 14, in pocket) may be divided into the following major structural units: Chimney Rock thrust-sheet, Whaleback duplex, Rice Creek horse, Rocking P horse and Cougar duplex. The Chimney Rock thrust probably ramps from a detachment at the top of the Fernie Formation to the upper detachment. The Chimney Rock thrust sheet dips steeply near the surface and is poorly imaged on seismic line WC1 (Figure 15, in pocket). Shallow-dipping portions of the thrust may be recognized at depth near the west edge of section WC1. The Whaleback duplex, partially eroded on section 1, consists of 6 horses with a floor thrust in the Wapiabi Formation and a roof thrust within the Bearpaw Formation. Strata in the fourth horse of this duplex have been involved in a fault propagation fold. The Rice Creek horse is underlain by the Rice Creek fault and overlain by the floor thrust of the Whaleback duplex.

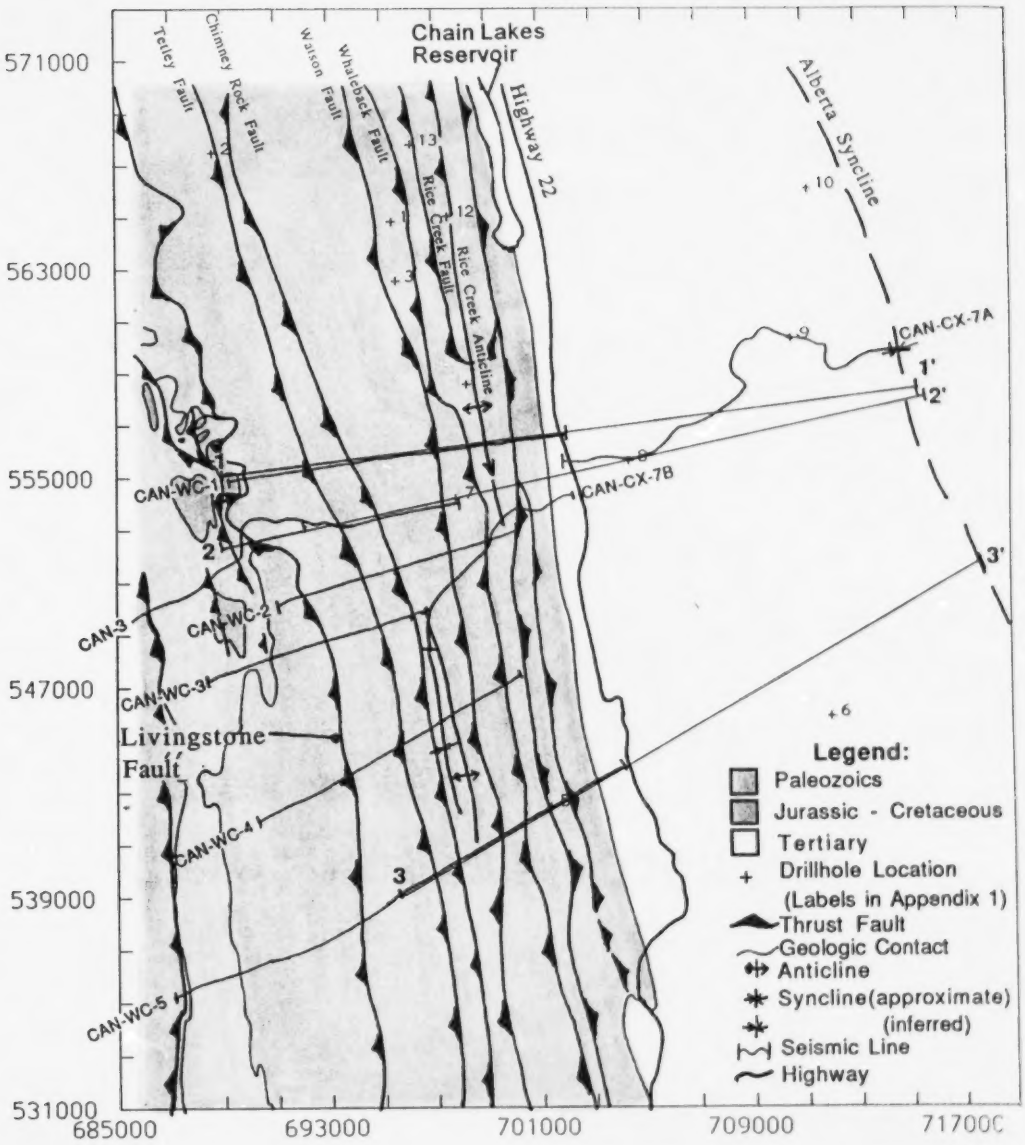

Figure 13: Map showing the position of cross sections 1, 2 and 3. Geology modified after Douglas (1950). Grid labels are UTM coordinates in metres.

The Rice Creek fault ramps at 19° - 20° from a basal detachment at the top of the Fernie Formation and flattens within the Blackstone Formation for approximately 5.7 km before ramping at a shallow angle (10° - 12°) to the Wapiabi Formation. It follows a short flat within the Wapiabi and ramps at 25° - 30° to the upper detachment. The Rocking P horse is underlain by the Rocking P thrust and overlain by the Rice Creek thrust. The Rocking P thrust ramps at 18 from the Exshaw to the Wapiabi Formations. It flattens within the Wapiabi before ramping to the upper detachment. A minor thrust with a detachment at the top of the Fernie Formation divides the Rocking P horse into two parts. A 0.1 to 0.2 second 'pull-up' of the near Cambrian reflector occurs due to the repetition of high velocity Mississippian carbonates in the hanging wall of the Rocking P thrust (A-B on section WC1). The Cougar duplex consists of 5 horses, with a floor thrust at the top of the Fernie Formation and the upper detachment as its roof thrust.

Except for the minor thrust in the Rocking P horse, deformation proceeded from hinterland to foreland. The restored positions of most major structures are shown on Figure 30 (in pocket). Displacement along the oldest structure, the Chimney Rock thrust, is unknown since the hangingwall cutoff has been eroded and the footwall cutoff occurs beyond the western edge of section 1. Figure 16 is a schematic diagram of the Whaleback duplex at the time of its formation; at least 13 km of displacement has occurred within this duplex. The Rice Creek thrust (Figure 17) displaced the Rice Creek horse approximately 2.6 km and folded the Chimney Rock thrust-sheet and Whaleback duplex. The Rocking P horse (Figure 18a) was transported 4.8 km toward the foreland by the Rocking P thrust. The Rocking P thrust was reactivated during formation of the Cougar duplex (Figure 18b). The 4 km cumulative displacement of the horses which comprise the Cougar duplex is equal to the width of the hangingwall flat of the Rocking P thrust at the top of the Fernie Formation.

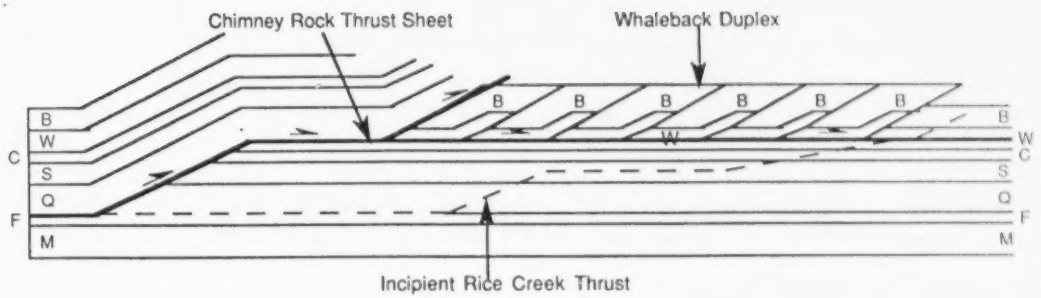

Figure 16: Schematic section of the Chimney Rock thrust-sheet, Whaleback duplex and incipient Rice Creek thrust. B = Belly River, W = Wapiabi, C = Cardium, S = Blackstone, Q = Blairmore, F = Fernie, M = Mississippian. Bold lines = active thrusts. Short dashed lines = folded or inactive thrusts. Long dashed lines = incipient thrusts.

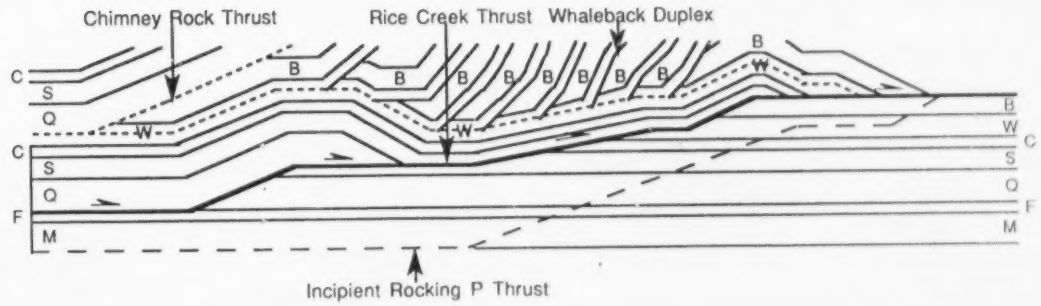

Figure 17: Schematic cross section of the Rice Creek thrust, folded Chimney Rock thrust, Whaleback duplex and incipient Rocking P thrust. See Figure 16 for legend.

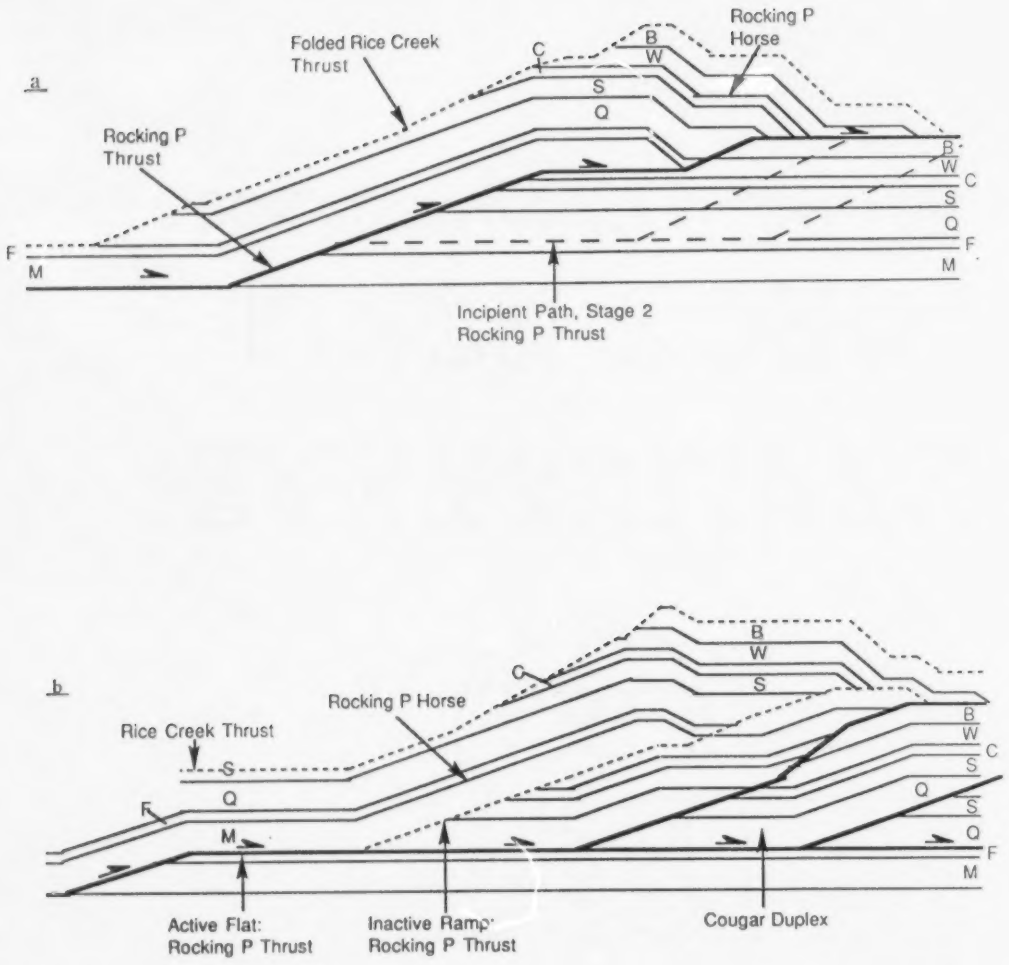

Figure 18: Schematic cross sections: a) Stage 1 (ramp stage) formation of the Rocking P horse, the incipient path for stage 2 of the Rocking P thrust. b) Stage 2 of the Rocking P thrust and the Cougar duplex. See Figure 16 for legend.

Section 2

The Chimney Rock thrust-sheet, Whaleback duplex, Rice Creek Horse and Cougar duplex are all recognizable on section 2 (Figure 19, in pocket). However, the Rocking P horse displays significant differences and an additional structural unit, the YL horse, is present. A proprietary seismic line (Can-3) was used to assist in the construction of this section. Seismic line WC2 (Figure 20, in pocket), is approximately 2 km south of section 2 and is sub-parallel to it; it is of poor quality but shows many of the major structures present on section 2 to the north and will be used for discussion purposes.

The Chimney Rock thrust-sheet is steeply dipping where it crops out on section 2. The underlying thrust probably ramps from the top of the Fernie Formation to the upper detachment. The Whaleback duplex occurs at a lower elevation on section 2 and, in contrast to section 1, the hangingwall cutoffs for three of its four horses have not been removed by erosion. The Rice Creek horse is very similar to that on section 1 (Figure 17). The Rocking P fault ramps at 24° from a basal detachment at the top of the Fernie Formation (vs. the Exshaw Formation on section 1), follows a short flat within the Wapiabi Formation and ramps to the upper detachment. The Rocking P horse is thinner here than on section 1 due to the absence of Mississippian strata. A minor out-of-anticline thrust occurs in the Rocking P horse. Strata of the YL horse overlie the YL thrust which ramps at 17° - 18° from a detachment in the Exshaw Formation to the top of the Fernie Formation. A pull-up of the near Cambrian reflector (A-B on seismic section WC2) occurs as a result of the duplication of Mississippian strata in the hangingwall of the YL thrust. The Cougar duplex consists of 4 horses, with a floor thrust at the top of the Fernie Formation and the upper detachment as its roof thrust (penetrated by wells 2-29-13-2W5 and 16-25-13-2W5). Strata in the western horse of the Cougar duplex are involved in a fault propagation fold, the forelimb of which has been cut by minor thrusts.

The Chimney Rock thrust-sheet, Whaleback duplex and Rice Creek horse developed in a very similar manner to their equivalents on section 1 (Figures 16,

17 and 31 (in map pocket)). Over 10 km of displacement has occurred within the Whaleback duplex. The Rice Creek thrust has transported strata in the Rice Creek horse 4 km toward the foreland. The Rocking P thrust (Figure 21a) transported the Rocking P horse 3.8 km toward the foreland. A lateral ramp in this fault occurs between sections 1 and 2 (see below). The YL thrust transports Mississippian strata in its hangingwall 3.6 km to the top of the Fernie Formation. Movement along this thrust folded the overlying Rocking P horse (Figure 21b). The Cougar duplex developed in front of the YL thrust: its cumulative displacement (3.8 km) approximately equals the displacement on the YL thrust.

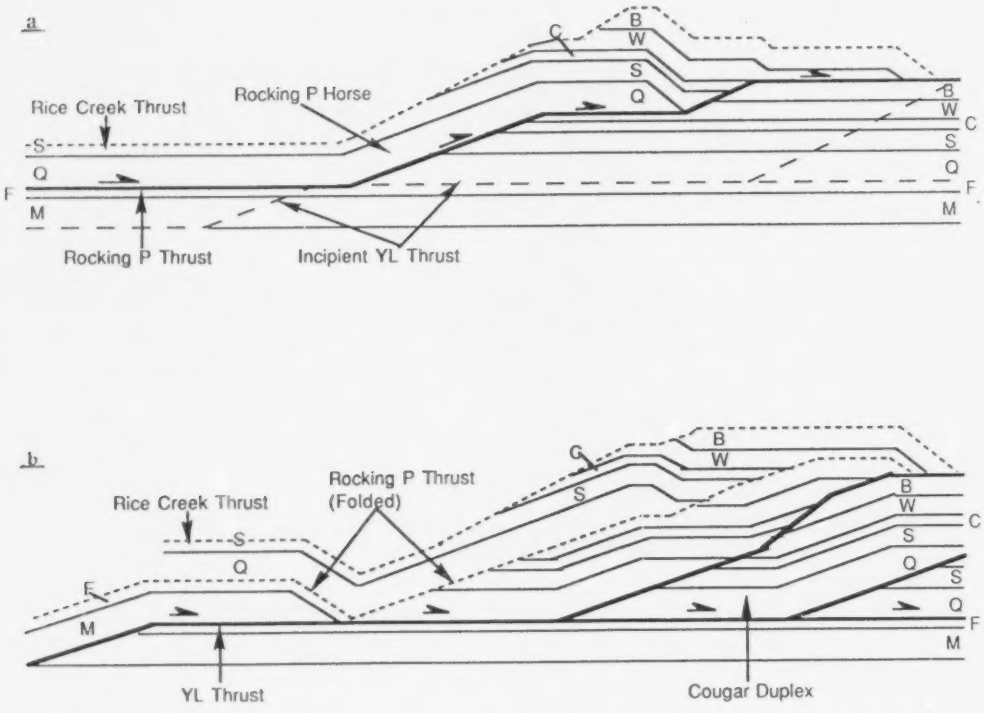

Figure 21: Schematic cross sections. a) The Rocking P thrust with folded Rice Creek and incipient YL thrusts. b) The YL thrust and Cougar duplex with the folded Rocking P thrust. See Figure 16 for legend.

Section 3

The structure on section 3 (Figure 22, in pocket) may be divided into the following major structural units: Chimney Rock thrust-sheet, Whaleback duplex, Rocking P horse and Cougar horse. The main difference between this section and the sections to the north is that deformation is restricted to the Mesozoic.

The Chimney Rock thrust-sheet is similar to that on sections 1 and 2, although the oldest unit to crop out is the Blackstone Formation and not the Blairmore Group. The Whaleback duplex consists of 6 horses, with a floor thrust in the Wapiabi Formation and the upper detachment as its roof thrust. Strata of the Rocking P horse are underlain by the Rocking P fault and overlain by the Whaleback duplex. The Rocking P fault ramps at approximately 30° from a detachment at the top of the Fernie Formation to the Wapiabi Formation and ramps at 20° to the upper detachment. A small out-of-anticline thrust has developed in the frontal fault bend fold of this horse. The Cougar horse consists of strata deformed above the Cougar fault. This thrust ramps at 10° from the top of the Fernie Formation to the upper detachment. Dipmeter data from well 15-15-12-1W5 and seismic data from seismic line WC5 (Figure 23, in pocket) confirm the low cutoff angle for this thrust.

Except for minor out-of-anticline thrusts in the Rocking P horse, deformation proceeded from hinterland to foreland (see restored section (Figure 30, in pocket)). The oldest structure, the Chimney Rock thrust probably ramps from a detachment at the top of the Fernie Formation to the Blackstone Formation, follows a flat within the Blackstone Formation and ramps to the upper detachment. Figure 24 is a schematic diagram of the Whaleback duplex at the time of its formation. Its horses are smaller and its displacement much less than on Sections 1 and 2 to the north. Strata within the Rocking P horse have been displaced by approximately 5 km. The youngest major thrust on this section, the Cougar thrust, has displaced the Blairmore Group approximately 5 km.

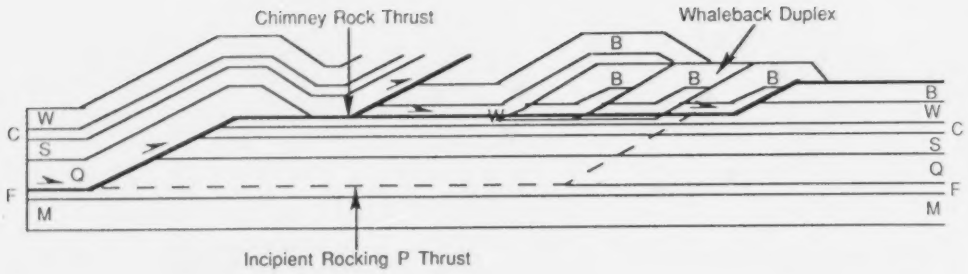

Figure 24: Schematic cross section of the Chimney Rock thrust-sheet and Whaleback duplex with the incipient Rocking P thrust. See Figure 16 for Legend.

Lateral Ramps

A major lateral ramp exists where the Rocking P thrust ramps parallel to its strike from a detachment in the Exshaw Formation along Section 1 to a detachment in the Fernie Formation along Section 2. Figure 25 shows the hanging wall cutoff for Mississippian strata which steps back 4 to 5 km to the west between Sections 1 and Section 2. On Section 1, Mississippian strata have been displaced 8.8 km by the Rocking P Fault. On Section 2 the Rocking P fault has approximately 4 km of displacement. Mississippian strata above the YL thrust have been displaced approximately 4 km along Section 2. This thrust has folded the overlying Rocking P thrust (Figure 21b). The cumulative displacement for the Rocking P and YL faults is approximately 8 km, similar to the total displacement (8.8 km) along the Rocking P thrust to the North (Section 1).

The events leading to the formation of the lateral ramp can be divided into two stages (Figure 26). Figure 26a shows the approximate geometry of the incipient lateral ramp. During the first stage, approximately 4 km of displacement occurred along the Rocking P thrust,

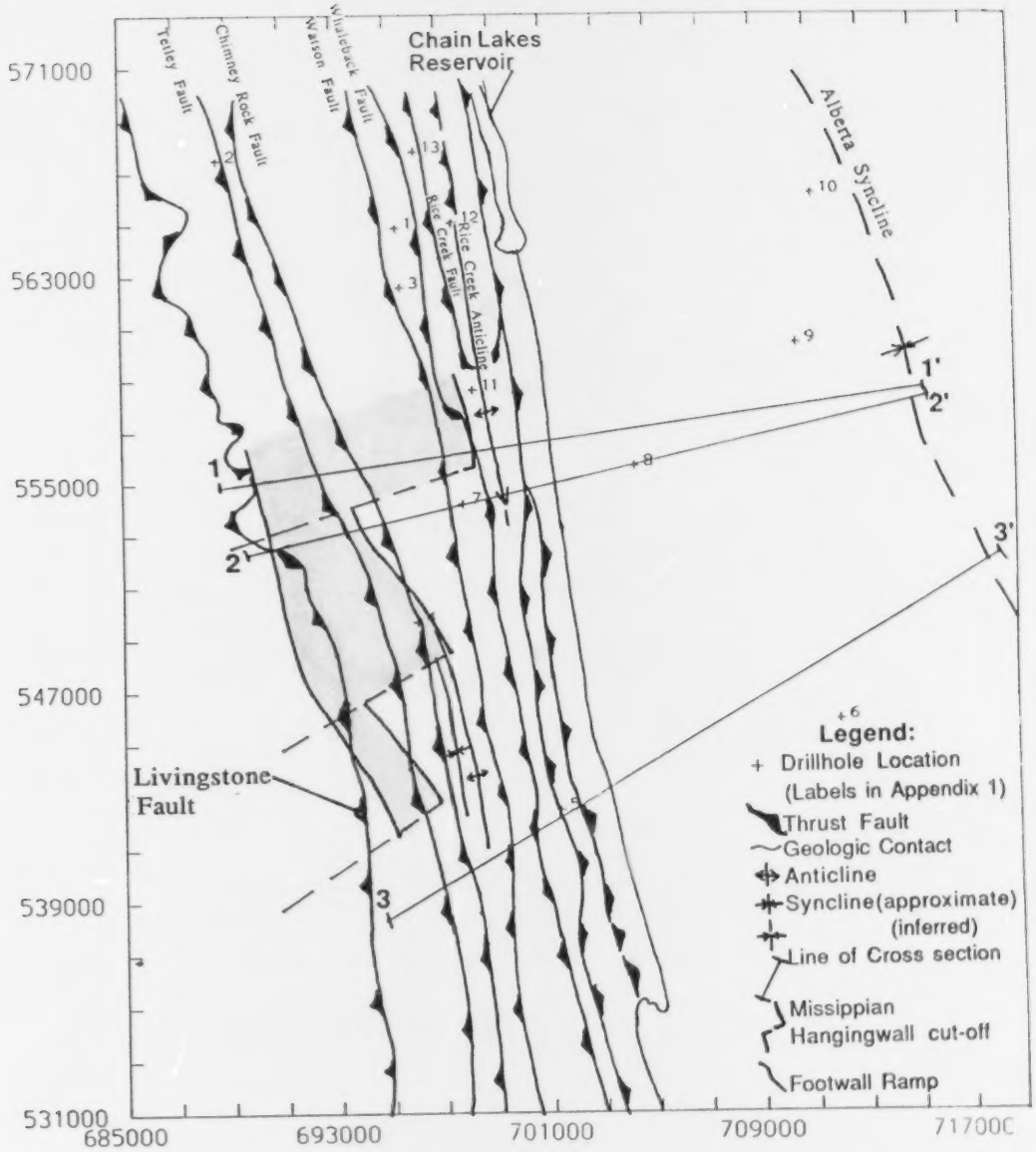

Figure 25: Map showing the hangingwall cut-off for Mississippian strata (shaded blue) and the position of the footwall ramps to the Rocking P and YL thrusts. Locations of cross sections 1, 2 and 3 are shown. Grid labels are UTM coordinates in metres. Geology modified after Douglas (1950).

transporting strata up a frontal ramp to the upper detachment (Figure 26b). A lateral ramp fold (McClay, 1992) has developed where Mississippian strata have been translated over the lateral ramp. This structure generates the 5° - 15° southerly plunge evident in the Rice Creek Anticline at surface. The shallow southerly plunge suggests that the lateral ramp likely dips at a shallow angle (10° - 15°) to the north-northwest. Figure 26b shows the footwall ramp position for the incipient YL thrust with a detachment in the Exshaw Formation. During the second stage in the history of the lateral ramp, the YL thrust transports Mississippian strata over a ramp to the top of the Fernie Formation where the fault flattens (Figure 26.3). This fault folds the overlying Rocking P thrust along Section 2 (Figure 21b). Mississippian strata are displaced by a similar amount during the second stage of deformation on the Rocking P thrust, forming the 4 km flat at the top of the Fernie Formation (Figure 18b). This sequence of events explains why a similar amount of total displacement occurs on the Rocking P thrust along Section 1 and the Rocking P thrust and the YL thrust along Section 2.

Bearpaw structure

Whereas strata beneath the Bearpaw Formation are cut by a complex system of foreland-verging thrusts, the overlying strata have a much simpler structure and lie in the west limb of the Alberta syncline. Thus, a zone of structural disharmony exists within the Bearpaw Formation (Plate 1). This zone is also a major detachment because all the thrusts that affect the underlying strata, with a total displacement of up to 25 km or more, merge within this zone. The vergence of this detachment is not immediately apparent and will be discussed below.

From the standpoint of large-scale structure, the Bearpaw Formation lies within the west limb of the Alberta syncline. Its small scale structure is likely to be extremely complex as indicated by the fact that it has everywhere been

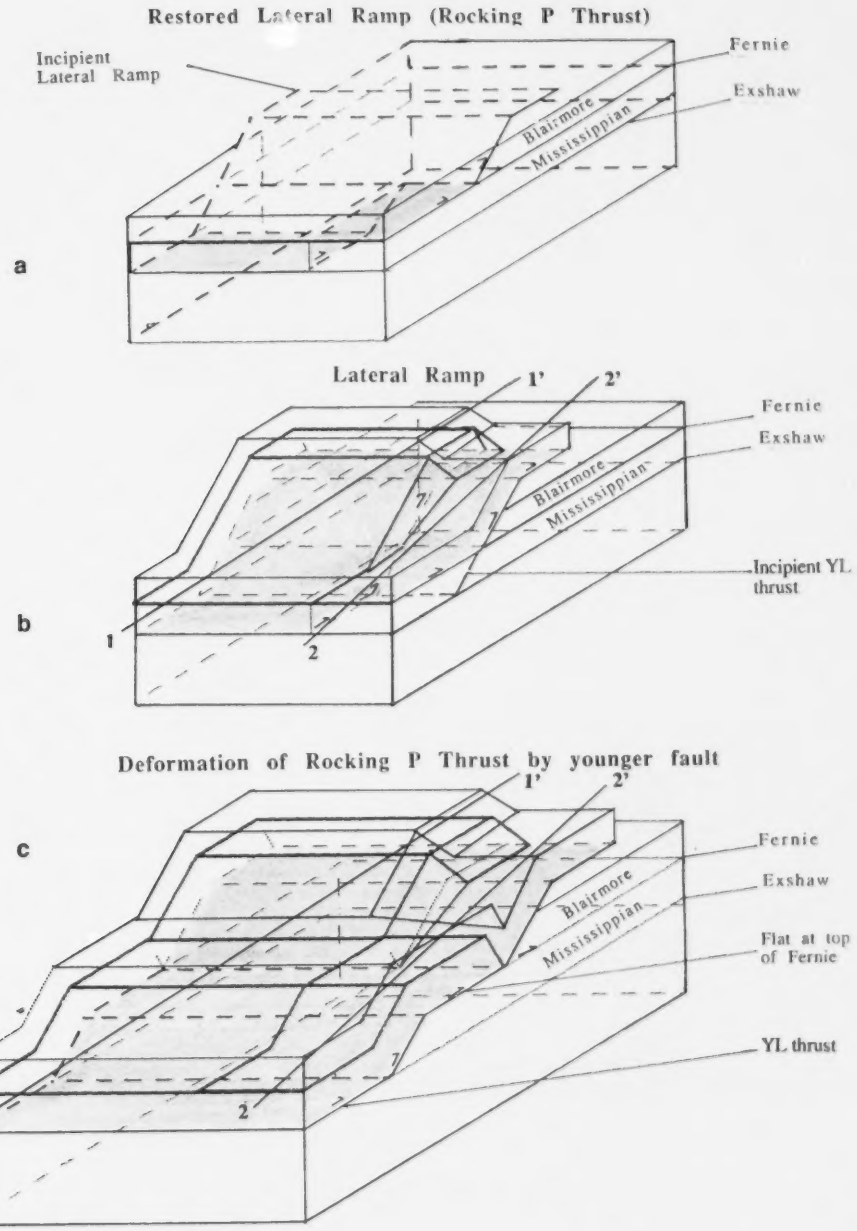

Figure 26: a) Incipient geometry of the lateral ramp formed where the Rocking P thrust ramps up-section to the south from the level of the Exshaw Formation to the top of the Fernie Formation. b) Translation of strata above the Rocking P fault over the lateral ramp results in the formation of a lateral ramp anticline with a southerly plunge. The approximate positions of cross sections 1 and 2 are shown. c) The YL thrust transports Mississippian strata to the top of the Fernie Formation, reactivating the Rocking P fault on section 1 (active fault surfaces are shaded grey). The lateral ramp for simplicity is shown as vertical but likely dips to the north at approximately 15°.

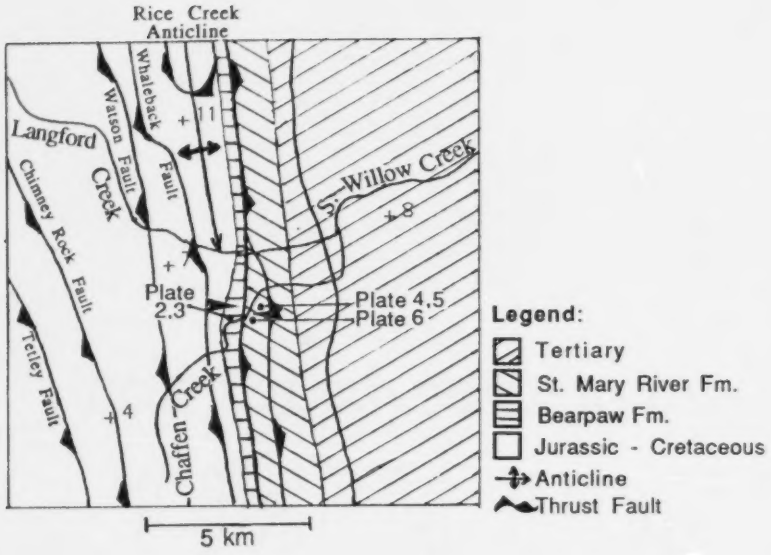

Figure 27: Map showing locations of plates 2 through 6 and vergence direction (Arrows) evident from mesoscopic structures at each location. Drillholes 7-7-13-2W5 (#4), 2-29-13-2W5 (#7), 1-4-14-2W5 (#11), and 16-25-13-2W5 (#8) are shown. Grid labels are UTM coordinates in metres. See Appendix 1 for drillhole identifiers.

tectonically thickened. On all three cross sections, the Bearpaw Formation has been structurally thickened up to 4 times its normal stratigraphic thickness. In well 15-15-12-1W5, located near the outcrop trace of the top of the upper detachment, drillhole data suggest that the Bearpaw Formation is 3 to 4 times its normal thickness. In wells 12-26-12-1W5, 10-10-14-1W5 and 16-25-13-2W5, located closer to the foreland, thickening of the Bearpaw Formation is less than two-fold. At one locality, mesoscopic folds in upper Bearpaw shales display foreland vergence (Plates 2 and 3; see Figure 27 for location).

Structure of the St. Mary River and younger Formations

Strata above the upper detachment belong to the St. Mary River, Willow Creek and Porcupine Hills Formations and lie in the west limb of the Alberta syncline. On Sections 1 and 2, the east dip of these strata decreases progressively eastward from a maximum of 55°, giving the top of the upper detachment a listric

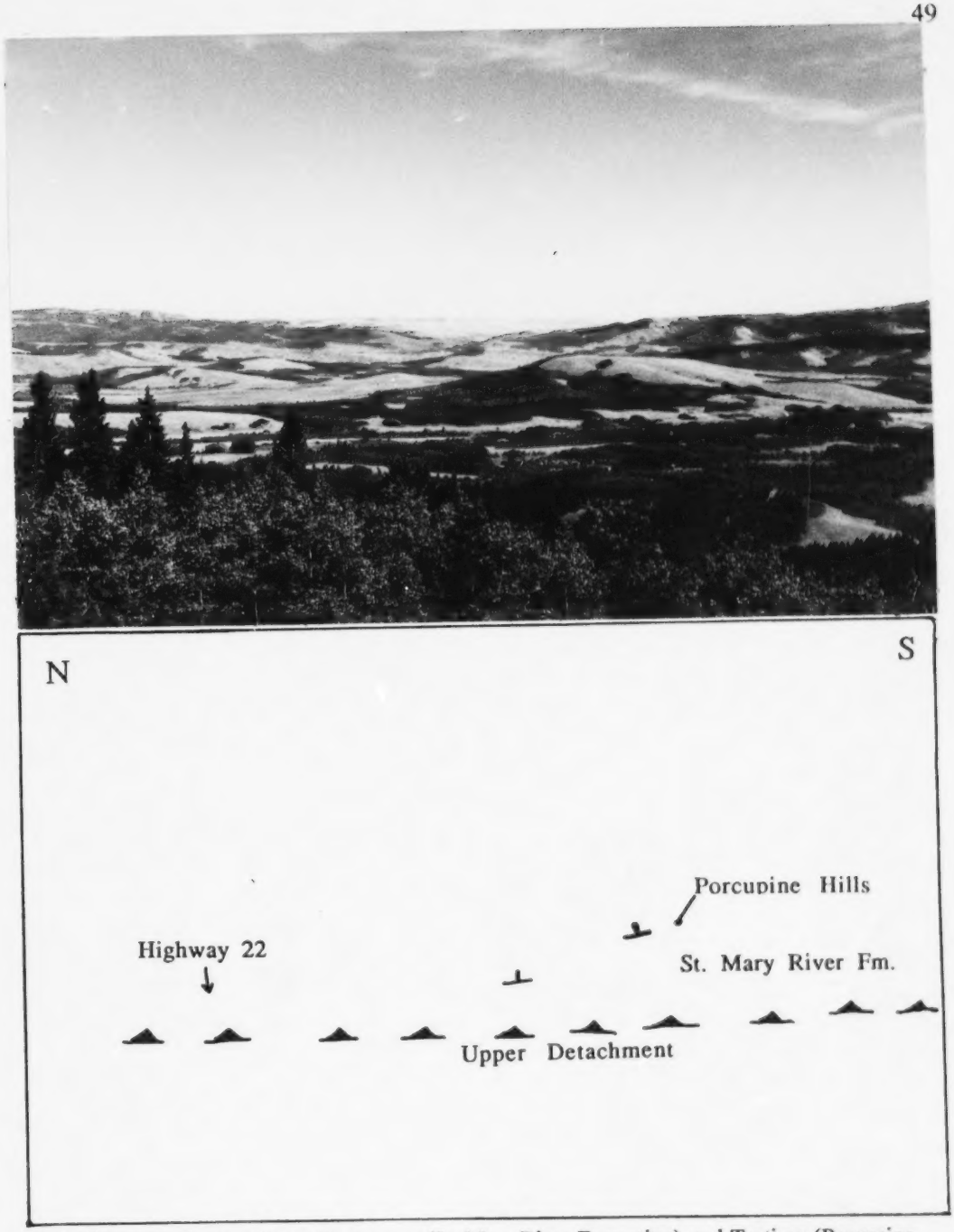

Plate 1: East dipping Upper Cretaceous (St. Mary River Formation) and Tertiary (Porcupine Hills and Willow Creek Formations) strata in the hangingwall of the upper detachment. The trace of the upper detachment occurs at or below the base of the St. Mary River Formation along the floor of the valley in the immediate foreground. Highway 922 is located in the next valley to the east. Photo taken facing east, from the top of the Rocking P anticline looking down the valley of South Willow Creek.

geometry. At two localities mesoscopic structures in the basal St. Mary River Formation display hinterland vergence (Plates 4, 5 and 6; see Figure 27 for location). On Section 3 the structure is similar but displays one major difference. St. Mary River strata have been duplicated by an east-dipping, west-verging thrust that ramps from the upper detachment to the base of the Willow Creek Formation.

On Section 3, the configuration of the top of the Willow Creek Formation is unclear. It is impossible to connect this horizon mapped at surface with that determined from chip samples in well 12-26-12-1W5 and at the same time honour the surface dips. Variations in stratigraphic thickness or facies changes may explain this anomaly.

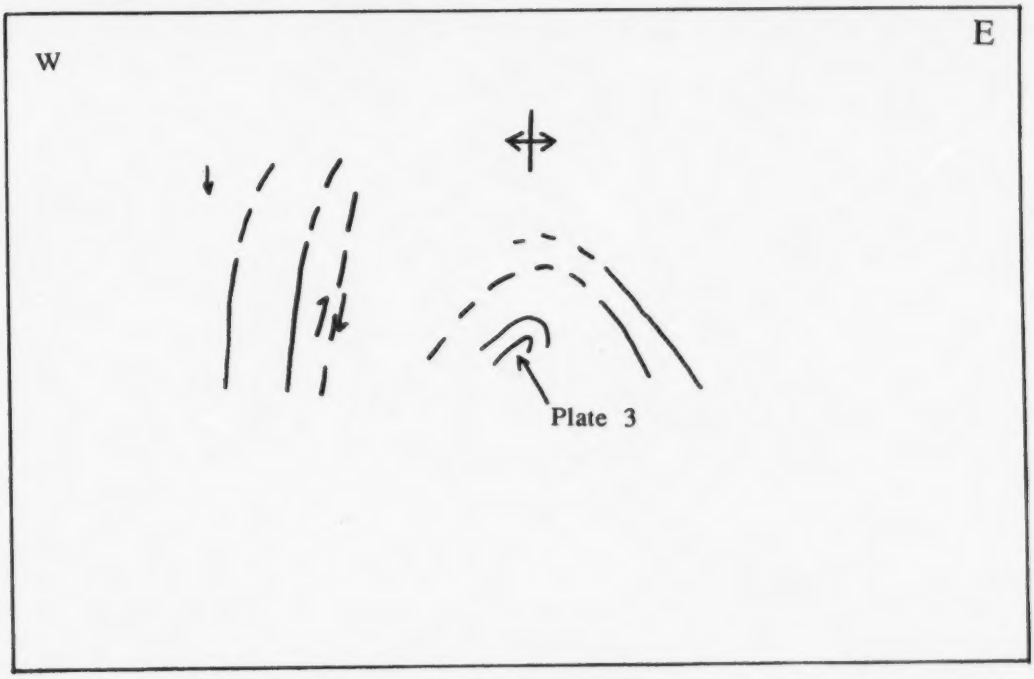

Plate 2: Faulted anticline in sandstones and shales of the Bearpaw Formation. Location of plate 3 is shown. The orange weathering sandstones have been rotated to vertical by deformation in underlying strata. View direction 344°, fence posts at the top of the ridge (Arrow) are approximately 1 m high.

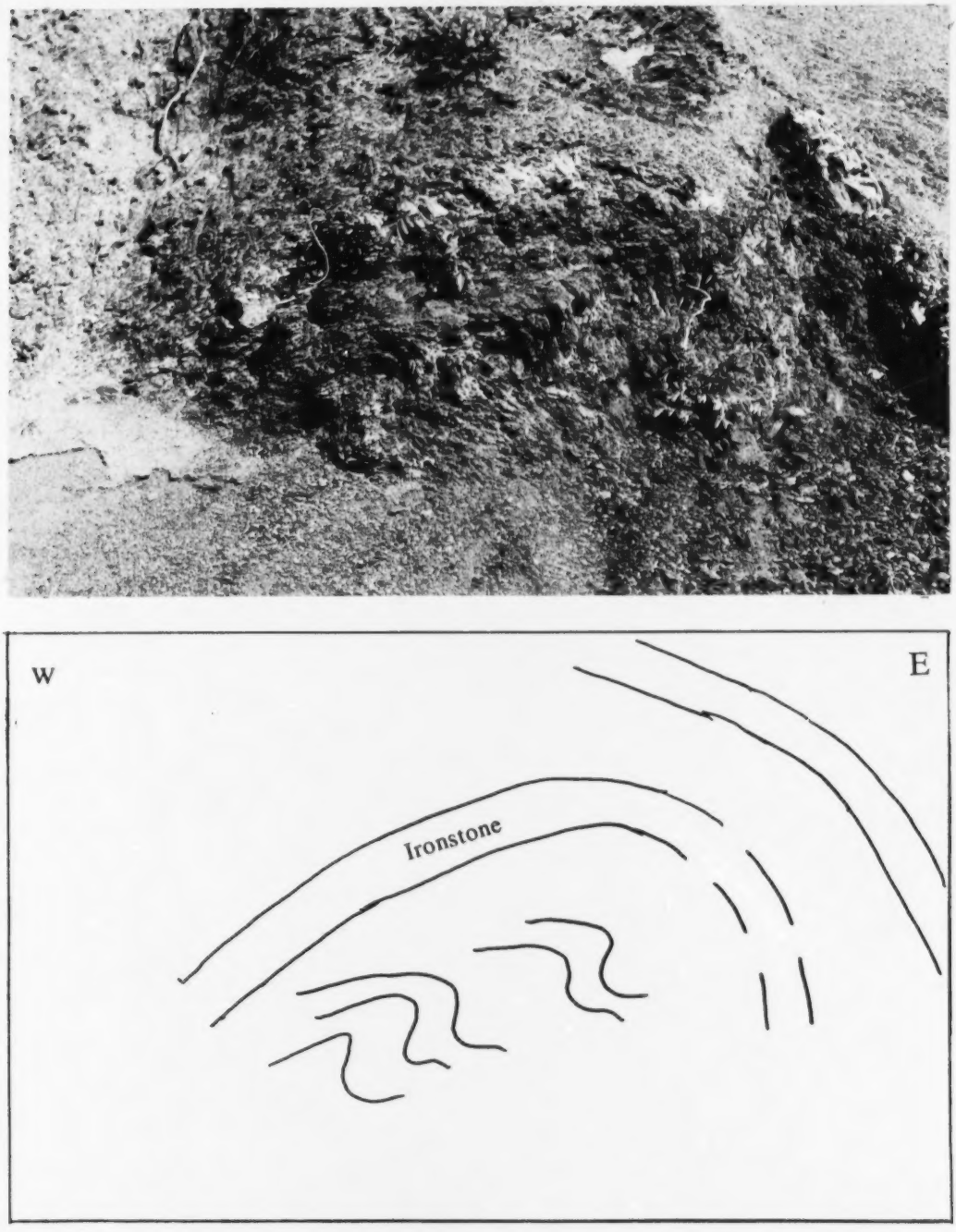

Plate 3: Asymmetric anticline developed in shales and ironstones of the Bearpaw Formation. Competent ironstone beds are concentrically folded; disharmonic folds in the core of the anticline plunge towards 310° at 26-32° and display foreland vergence (east). Field of view approximately 2 m, view direction 344°.

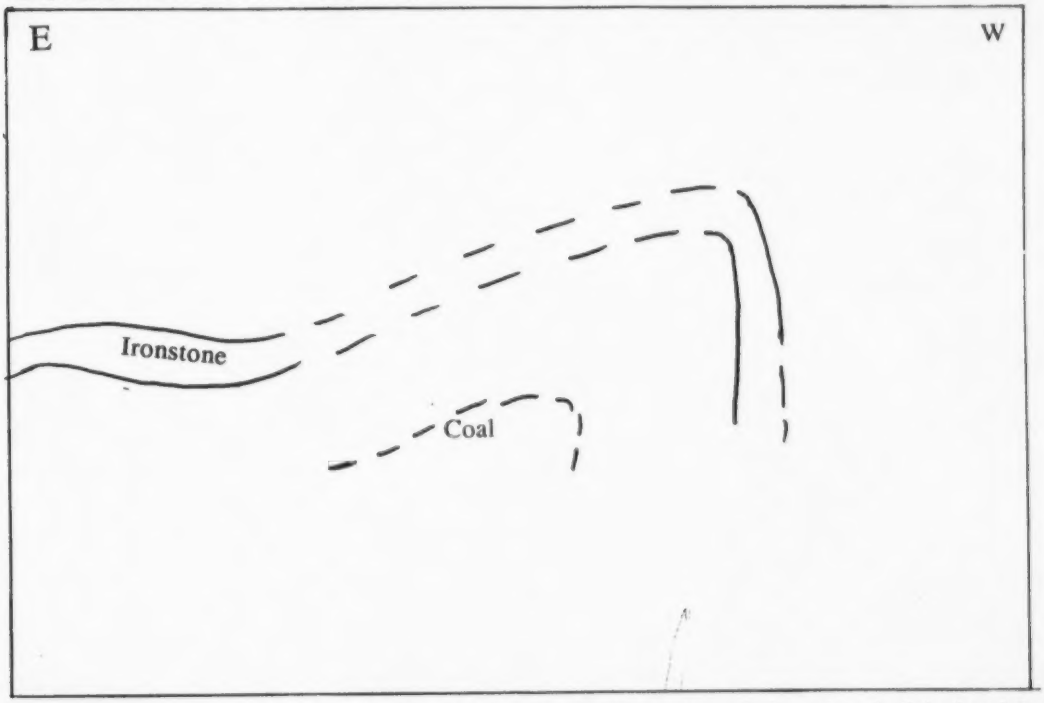

Plate 4: Fault propagation fold developed in interbedded ironstone, shale and coal of the basal St. Mary River Formation. Coal occupies the core of the fault propagation fold. Beds in the west limb of the fold. are vertical to overturned. The sense of vergence for the fold is toward the hinterland (West). View direction 199°; bushes in the foreground are approximately 1 m high.

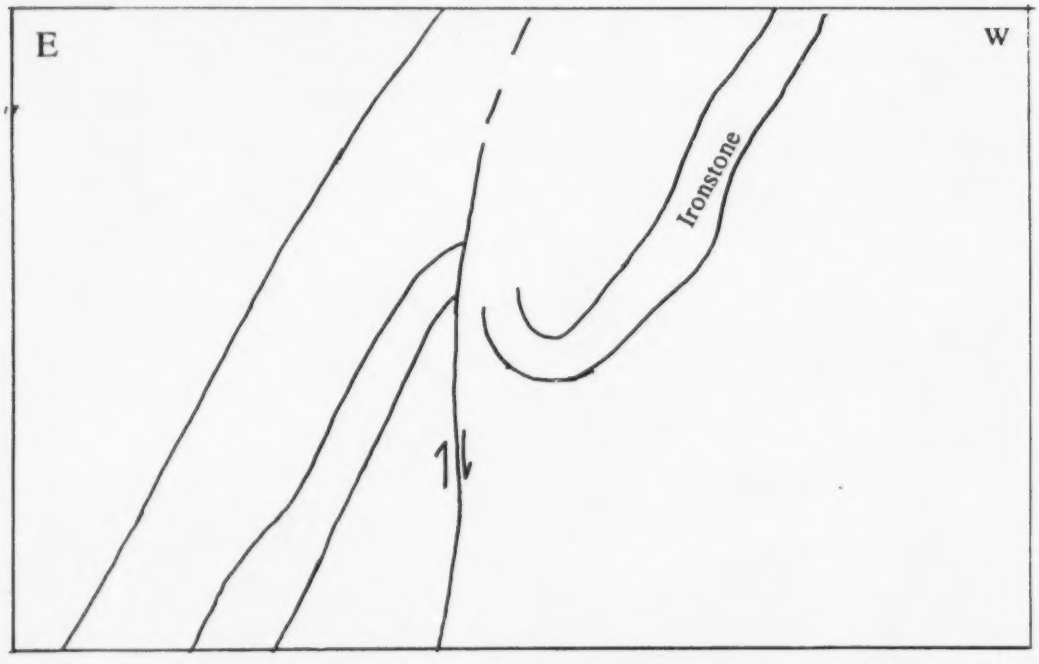

Plate 5: Minor structure developed on the east limb of the fault propagation fold of plate 4. A fault ramps up from a bedding plane detachment in the shales beneath the orange-brown ironstone (cut by the fault) to shales above the ironstone bed. Displacement on this minor thrust is toward the hinterland (West). View direction 160°.

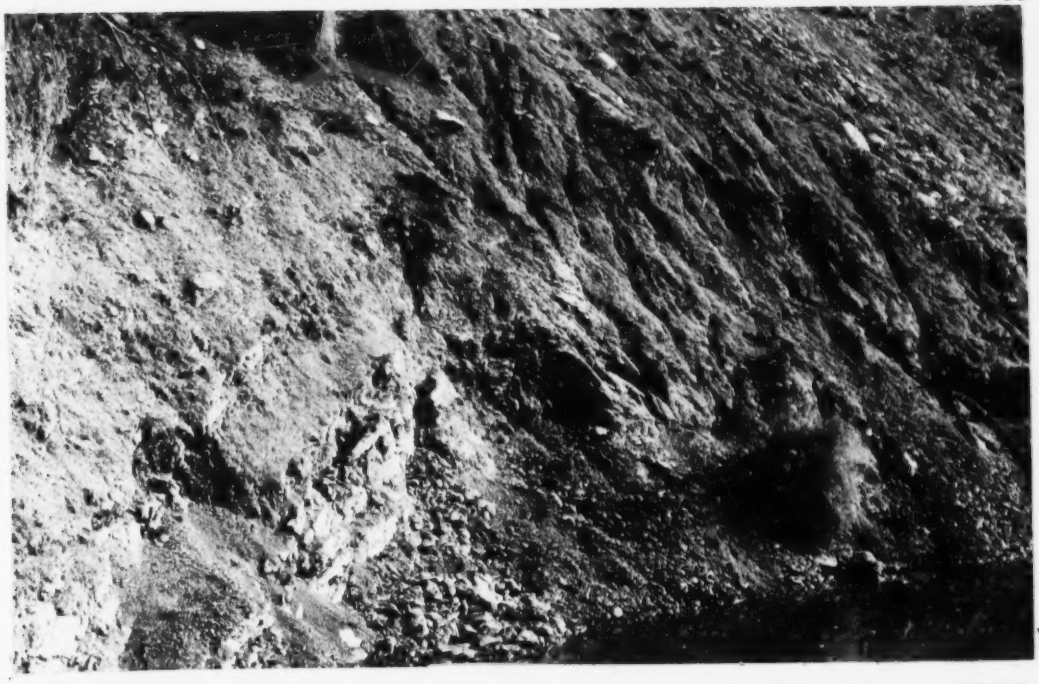

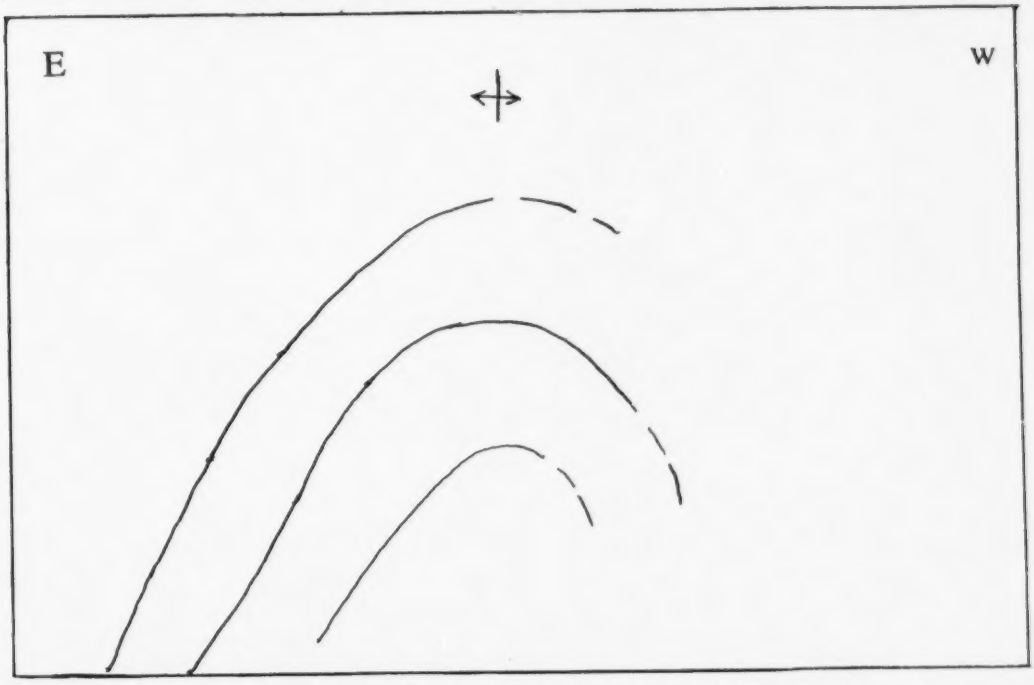

Plate 6: Asymmetric anticline developed in strata of the basal St. Mary River Formation. The structure is more asymmetric than is apparent from the perspective of this photo. The east limb of this structure flattens abruptly immediately east of this photo and is much broader than the west limb. The vergence is toward the hinterland (West). View direction 182°, clump of grass near the base of the cliff is approximately 30 cm high.

Structural synthesis

The structure of strata between the basal and upper detachments is dominated by foreland verging thrusts, with a total displacement of up to 25 km. The displacement along each of these thrusts decreases towards the foreland due to fault-bend folding. The magnitude of this decrease is controlled by such factors as the number of ramps between the basal and upper detachments and the fundamental cutoff angles. As a result, the total foreland verging displacement transferred to the upper detachment may be significantly less than 25 km.

Deformation beneath the foreland, i.e. in this case beyond the axial trace of the Alberta syncline, used to be regarded as negligible. This view is now known to be incorrect. Displacement along a detachment beneath the foreland can be taken up by layer parallel shortening in the overlying strata (Hatcher et al., 1989). Contractional strains of up to 30% have been proposed for strata beneath the Appalachian Plateau Province (Bowen, 1986; Dean and Kulander, 1972; Engelder and Engelder, 1977; Nickelsen, 1966). Deformation is known to occur at least 50 km east of the axial trace of the Alberta syncline (Skuce et al., 1992). Thus, much of the foreland verging displacement transferred to the upper detachment from underlying thrusts in the outer foothills may continue into the foreland and be dissipated by layer parallel shortening in strata above the Bearpaw Formation (Figure 28). The vergence of the upper detachment during this stage would be toward the foreland. Nevertheless, many of the thrusts entering the upper detachment, for at least part of their history, seem to have ended against hinterland verging thrusts such as that responsible for the duplication of the St. Mary River Formation along Section 3, which has at least 2 km of displacement.

The competent nature of the St. Mary River Formation accounts for the smooth, regular configuration of the top of the upper detachment. The configuration of the base of the upper detachment on the other hand is extremely irregular owing to the existence of ramp anticlines involving Belly River strata. To accommodate the difference between the shapes of the top and bottom of the

upper detachment, the Bearpaw Formation experienced considerable small scale deformation and tectonic thickening (Figure 29).

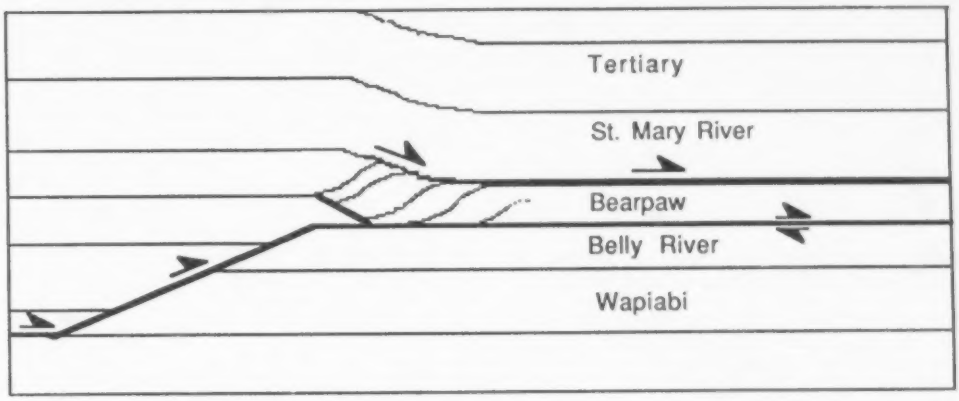

Figure 28: Schematic diagram of initial stages of structural thickening within the upper detachment zone. Displacement in strata above the upper detachment is dissipated by layer parallel shortening giving the upper detachment foreland vergence.

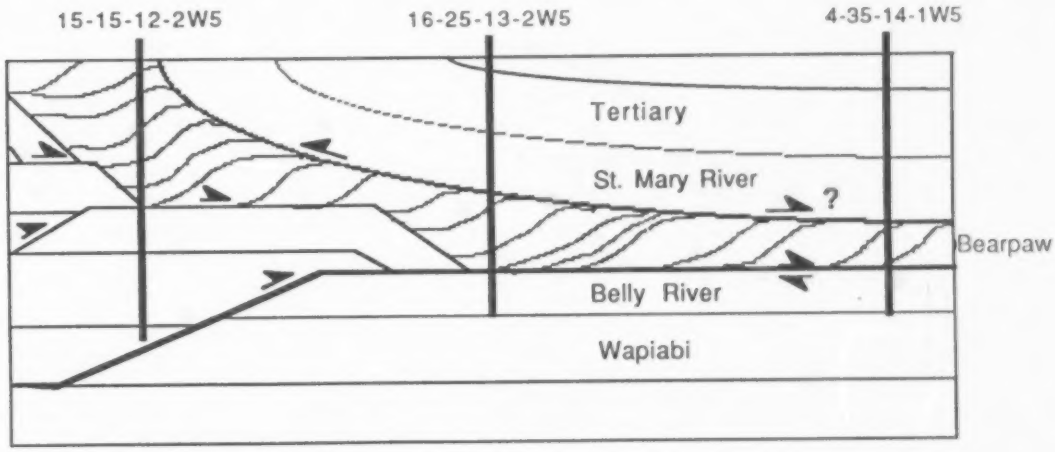

Figure 29: Schematic section of later stages of structural thickening within the upper detachment zone, with displacement transferred to the surface along a hinterland verging thrust. Diagram shows the approximate position of drillholes within the study area, relative to the outcrop trace of the upper detachment. Structural thickening of Bearpaw formation strata within these wells decreases eastward. The upper detachment follows a smooth geometry above these thickened strata.

CHAPTER 8
SUMMARY AND CONCLUSIONS

From a structural standpoint, three lithotectonic units may be distinguished: 1) Mississippian to Belly River strata deformed by foreland verging thrusts, 2) the internally deformed and tectonically thickened Bearpaw Formation and 3) St. Mary River and younger strata in the west limb of the Alberta syncline. A major lateral ramp affects strata belonging to the lowest lithotectonic unit. This ramp connects flats in the Exshaw and Fernie Formations. The lateral ramp anticline that developed in strata translated over this structure is responsible for the 5 - 15° southerly plunge of the Rice Creek Anticline. Most foreland verging thrusts in the lower lithotectonic unit flatten within the upper detachment, the base of which is irregular due to the presence of ramp anticlines involving Belly River strata. East dipping strata above the upper detachment shallow progressively eastward, displaying a listric geometry. To accommodate the difference in shape between these two horizons, strata of the Bearpaw Formation have experienced complex internal deformation and structural thickening. Displacement associated with foreland verging thrusts below the upper detachment continues 50 km or more into the foreland, and is dissipated by layer parallel shortening in units which overlie the upper detachment and in part is transmitted to the surface along hinterland verging backthrusts.

REFERENCES

Aitken, J.D., 1989. The Sauk Sequence - Cambrian to Lower Ordovician Miogeocline and Platform. *In*: Rickets, B. D. (ed.) Western Canada Sedimentary Basin. A Case History. Canadian Society of Petroleum Geologists. 320 pages.

Bally, A. W., Gordy, P. L. and Stewart, G.A., 1966. Structure, Seismic Data and Orogenic Evolution of the Southern Canadian Rocky Mountains. Bulletin of Canadian Petroleum Geology. v. 14, p. 337-381

Bengston, C.A., 1981. Statistical Curvature Analysis Techniques for Structural Interpretation of Dipmeter Data. American Association of Petroleum Geologists Bulletin, v. 65, p. 312-332.

Bengston, C.A., 1982. Structural and Stratigraphic Uses of Dip Profiles in Petroleum Exploration. *In*: Halbouty, T. M. (ed.) The Deliberate Search for the Subtle Trap. American Association of Petroleum Geologists Memoir 32. p. 31-45.

Bossart, D. O., 1957. Relationship of the Porcupine Hills to Early Laramide Movements. *In*: Alberta Society of Petroleum Geologists 7th Annual Field Conference Guidebook. p. 46 -51.

Bowen, J.H., 1986. Regional Finite Strain Analysis of Basal Devonian Orthoquartzites: Valley and Ridge Province, Pennsylvania (M.Sc. thesis): Stores, University of Connecticut, 45 p. *Cited in*: Hatcher et al., 1989.

Caldwell, W.G.E., 1990. The Bearpaw Formation. *In*: D. J. Glass. (Ed.) Lexicon of Western Canadian Stratigraphy, Volume 4, Western Canada. Canadian Society of Petroleum Geologists. p. 74-75.

Charlesworth, H.A.K., Langenburg, C.W. and Ramsden, J., 1976. Determining Axes, Axial Planes and Sections of Macroscopic Folds using Computer-based Methods. Canadian Journal of Earth Sciences. v. 13, p. 54-65.

Charlesworth, H.A.K. and Gagnon, L.G., 1985. Intercutaneous Wedges, the Triangle Zone, and Structural Thickening of the Mynheer Coal Seam at Coal Valley in the Rocky Mountain Foothills of Central Alberta. Bulletin of Canadian Petroleum Geology, v. 33, p. 22-30.

Charlesworth, H.A.K., Johnston, S.T. and Gagnon, L.G., 1987. Evolution of the Triangle Zone in the Rocky Mountain Foothills near Coalspur, Central Alberta. Canadian Journal of Earth Sciences, v. 28, no. 8, p. 1668-1678.

Charlesworth, H.A.K, Guidos, J., Gold, C. and Wynne, D., 1989. Tripod 4.00, a Microcomputer Program for Storing, Retrieving and Analysing Orientations, Stratigraphic and Positional Data from Drillholes, Outcrops and Seismic Lines. GAIA Software Incorporated, Calgary.

Charlesworth, H.A.K. and Jahans, P.C., 1991. ORIENT: A Program to Analyze and Display Orientations. Department of Geology, University of Alberta.

Charlesworth, H.A.K., 1992. PENDNQ, a Microcomputer Program to reduce dipmeter readings. Department of Geology, University of Alberta.

Clark, L. M., 1954. Cross Section through the Clark Range of the Rocky Mountains of Southern Alberta and Southern British Columbia. *In*: Alberta Society of Petroleum Geologists 4th Annual Field Conference. p. 105-109.

Cruden, D.M. and Charlesworth, H.A.K., 1966. The Mississippian-Jurassic Unconformity near Nordegg, Alberta. Bulletin of Canadian Petroleum Geology. v. 14, p. 266-272.

Dahlstrom, C.D.A., 1970. Structural Geology of the Eastern Margin of the Canadian Rocky Mountains. Bulletin of Canadian Petroleum Geology, v. 18, p. 332-406.

Dawson, G.M., 1883. Report on the Country in the Vicinity of the Bow and Belly River Region, N. W. Territory. Geological Survey of Canada, Report of Progress, 1880-81-82, Part B.

Dean, S.L. and Kulander, B.R., 1972. Oolite Deformation Associated with Faulting in the Northern Shenendoah Valley. *In* P. Lessing, R.I. Hayhurst, J.A. Barlow and L.D. Woodfork, (Ed). Appalachian Structures Origin, Evolution and Possible Potential for new Exploration Frontiers: West Virginia Geological and Economic Survey, p. 103-139.

Dobrin, M.D. and Savit, C.H., 1988. Introduction to Geophysical Prospecting, Fourth Edition. McGraw-Hill Book Company, New York. 867 pages.

Douglas, R.J.W., 1949a. Gap, Alberta. Geological Survey of Canada Map 978A.

Douglas, R.J.W., 1949b. Callum Creek, Alberta. Geological Survey of Canada Map 982A.

Douglas, R.J.W., 1949c. Langford Creek, Alberta. Geological Survey of Canada Map 981A.

Douglas, R.J.W., 1950. Callum Creek, Langford Creek, and Gap Map Areas, Alberta. Geological Survey of Canada, Memoir 255. 124 pages.

Dwyer, M.K., 1986. The Geometry and Mechanical Development of Hanging Wall Structures of the Livingstone Thrust Fault, Alberta Foothills. M.Sc. Thesis, Department of Geology and Geophysics, University of Calgary. 166 pages.

Engelder, J.T. and Engelder, R., 1977. Fossil Distortion and Decollement Tectonics on the Appalachian Plateau. Geology, v. 5, p. 457-460.

Fallot, P., 1949. Les Chevauchements Intercutanes de Roya (A.-M.). Annales Hebert et Haug, Laboratoire Geologique, Universite de Paris, v. 7, p. 161-170.

Gordy, P.L., Frey, F.R. and Norris, D.K., 1977. Geological Guidebook for the Canadian Society of Petroleum Geologists and 1977 Waterton - Glacier Park Field Conference: Canadian Society of Petroleum Geologists, Calgary, 93 pages.

Guidos, J. 1991. EZDIGIT Version 1.01, A General Purpose Digitizer Interface Program. GAIA Software Incorporated, Calgary

Hake, B.F., Willis, R. and Addison, C.C., 1942. Folded Thrust Faults in the Foothills of Alberta. Bulletin of the Geological Association of America. v. 53, p. 291-334.

Hatcher., R.D. Jr., Thomas, W.A., Geiser, P.A., Snoke, A.W., Mosher, S. and Wiltschko, D.V., 1989. Alleghanian Orogen. *In* The Geology of North America. v. F2, The Appalachian-Ouachita Orogen in the United States. The Geological Society of America. p. 233-318.

Hatcher, R.D. Jr., 1990. Structural Geology; Principles, Concepts and Problems. Merill Publishing Company, Columbus, 531 pages.

Hood, P., 1981. Migration. *In*: Fitch, A.A. (Ed.) Developments in Geophysical Exploration Methods - 2, Elsevier Applied Science Publications. p 151-230.

Hume, G.S., 1940. Stimson Creek Map Area. Geological Survey of Canada, Map 934A.

Jamison, W.R., 1987. Geometric Analysis of Fold Development in Overthrust Terranes. Journal of Structural Geology, v. 9, n. 2, p. 207-220.

Jones, P.B., 1982. Oil and Gas beneath East-Dipping Underthrusts in the Alberta Foothills. *In*: R.B. Powers (Ed.) Geological Studies in the Cordilleran Thrust Belt. Denver, Rocky Mountain Association ofPetroleum Geologists, v. 1, p. 31-38.

MacKay, P.A., 1991. A Geometric, Kinematic and Dynamic Analysis of the Structural Geology at Turner Valley, Alberta. Unpublished Ph.D. Thesis, Department of Geology and Geophysics, The University of Calgary, Calgary, Alberta. 138 pages.

McClay, K.R., 1992. Glossary of Thrust Tectonic Terms. *In*: D.J. McClay (Ed.) Thrust Tectonics. Chapman and Hall. 447 pages.

McLean, J.R., 1977. The Cadomin Formation: Stratigraphy, Sedimentation, and Tectonic Implications. Bulletin of Canadian Petroleum Geology, v. 24, no. 4, p. 792-827.

McLean, J.R., 1990a. The Blairmore Group.
In: D. J. Glass. (Ed.) Lexicon of Western Canadian Stratigraphy, Volume 4, Western Canada. Canadian Society of Petroleum Geologists. p. 74-75.

McLean, J.R., 1990b. The Gladstone Formation.
In: D. J. Glass. (Ed.) Lexicon of Western Canadian Stratigraphy, Volume 4, Western Canada. Canadian Society of Petroleum Geologists. p. 257-258.

McQuillin, R., Bacon, M. and Barclay, W., 1984. An Introduction to Seismic Interpretation. Reflection Seismics in Petroleum Exploration. Graham and Trotman, 287 pages.

Mitra, S. and Namson, J. 1990. Balanced Cross Sections in Hydrocarbon Exploration and Production. American Association of Petroleum Geologists Short Course Notes.

Neidell, N. S., 1979. Stratigraphic Modelling and Interpretation of Geophysical Principles and Techniques. American Association of Petroleum Geologists, Education Course Notes Series #13, p. 2-9.

Nelson, H.W. and Glaister, R.P., 1983. Trap Creek Basal Belly River Section A Deltaic PrograditionalSequence. *In*: Sedimentology of the Upper Cretaceous Fluviatile, Deltaic and Shoreline Deposits, Southwestern Alberta Foothills. The Mesozoic of Middle North America Field Trip Guidebook no. 3, Canadian Society of Petroleum Geologists.

Nickelsen, R.P., 1966. Fossil Distortion and Penetrative Rock Deformation in the Appalachian Basin. Journal of Geology, v. 74, p. 924-931.

Norris, D.K., 1958. Livingstone River, Alberta. Geological Survey of Canada Map 5-1958.

Oswald, D.H., 1964. Mississippian Stratigraphy of South-Eastern British Columbia. Bulletin of Canadian Petroleum Geology, v. 12, p. 452-459.

Peterson, R.A., Fillipone, W.R., and Coker, F.B., 1955. The Synthesis of Seismograms from Well Logs. Geophysics, v. 20, n. 3, p. 516-538.

Price, R. A., 1981. The Cordilleran Thrust and Fold Belt in the Southern Canadian Rocky Mountains. *In*: Thrust and Nappe Tectonics. Geological Society of London, Special Publication #9.

Ramsay, J.G. and Huber, M.I., 1987. The Techniques of Modern Structural Geology. Volume 2: Folds and Fractures. Academic Press, London. 700 pages.

Robinson, E. A., 1983. Migration of Geophysical Data. International Human Resources Development Corporation. 208 pages.

Robinson, E.S. and Coruh, C., 1988. Basic Exploration Geophysics. John Wiley and Sons, New York. 562 pages.

Skuce, A.G., Goody, N.P. and Maloney, J., 1992. Passive Roof Duplexes under the Rocky Mountain Foreland Basin, Alberta. American Association of Petroleum Geologists Bulletin. v. 76, n. 1, p. 67-80.

Suppe, J., 1983. Geometry and Kinematics of fault-bend folding. American Journal of Science, v. 283, p. 684-721.

Suppe, J. and Chang, Y.L., 1983. Kink Method Applied to Structural Interpretation of Seismic Sections, Western Taiwan. Petroleum Geology of Taiwan, n. 19, p. 29-49.

Stott, D.F., 1963. The Cretaceous Alberta Group and Equivalent Rocks, Rocky Mountain Foothills, Alberta. Geological Survey of Canada, Memoir 317.

Stott, D.F., 1990a. The Blackstone Formation. *In*: D. J. Glass. (Ed.) Lexicon of Western Canadian Stratigraphy, Volume 4, Western Canada. Canadian Society of Petroleum Geologists. p. 73-74

Stott, D.F., 1990b. The Wapiabi Formation. *In*: D. J. Glass. (Ed.) Lexicon of Western Canadian Stratigraphy, Volume 4, Western Canada. Canadian Society of Petroleum Geologists. p. 502

Turner, D.R., 1990. The Porcupine Hills Formation. *In*: D. J. Glass. (Ed.) Lexicon of Western Canadian Stratigraphy, Volume 4, Western Canada. Canadian Society of Petroleum Geologists. p. 502

Wall, J.H. and Rosene, R.K., 1977. Upper Cretaceous Stratigraphy and Micropaleontology of the Crowsnest Pass - Waterton Area, Southern Alberta Foothills. Bulletin of Canadian Petroleum Geology, v. 25, n. 4, p. 842-867.

Wall, J.H. and Russel, L.S., 1990. The St. Mary River Formation. *In*: D. J. Glass. (Ed.) Lexicon of Western Canadian Stratigraphy, Volume. 4, Western Canada. Canadian Society of Petroleum Geologists. p. 600-601.

Wall, J.H., Russel, L.S, and Monahan, P.A., 1990. The Willow Creek Formation. *In*: D. J. Glass. (Ed.) Lexicon of Western Canadian Stratigraphy, Volume. 4, Western Canada. Canadian Society of Petroleum Geologists. p. 600-601.

Woodcock, N.H., 1977. Specification of Fabric Shape using an Eigenvalue Method. Geological Society of America Bulletin, v. 88, p. 1231-1236.

Woodward, N.B., Boyer, S.E. and Suppe, J., 1983. An Outline of Balanced Cross Sections. University of Tennessee Department of Geological Sciences Studies in Geology #11, 2nd. Edition.

Wuenschal, P.C., 1960. Seismogram Synthesis Including Multiples and Transmission coefficients. Geophysics, v. 25, p. 106-129.

Zaitlin, B.A., 1983. Sedimentology of the St. Mary River Formation at the Oldman River Bridge Crossing. *In*: Sedimentology of the Upper Cretaceous Fluviatile, Deltaic and Shoreline Deposits, Southwester Alberta Foothills. The Mesozoic of Middle North America Field Trip Guidebook n. 3, Canadian Society of Petroleum Geologists.

APPENDIX 1

ASCII data file format for Outcrops and Drillholes

Outcrop data ASCII file structure:

Primary Outcrop Record:

A	B	C	D	E	F	G
0	1	710735.4	540612.0	1615.5	T	R

A: Data record type: 0 = primary outcrop record
B: Outcrop Identification number
C: Easting
D: Northing
E: Elevation
F: Horizon Code: (one or two characters)
G: Way up: R - right way up, O - overturned, N - not known

Secondary Outcrop Records:

A	B	C	D	E	F	G	H
1	2	0	0	0	N	101	27
2	2	0	0	0	N	250	46 260 67 270 75

A: Data Record type:
1 - Bedding
2 - Mesoscopic fold, bedding folded at the scale of outcrop
B: Outcrop identification number
C: Pitch (real number between 0 and 180)
D and E: Axial Trace; two numbers specifying the trend and plunge in degrees of the axial plane of a mesoscopic fold.
F: Sense: U - Hanging wall up, D - hanging wall down, N - not known
G and H: Measurements; real numbers giving dip direction and dip in degrees, up to 8 measurements permitted.

Drillhole data ASCII file structure:

Primary Drillhole Records:

A	B	C	D	E	F	G	H	I	J
8	1	695415.4	564845.5	1437.7	0.0	90.0	4508.0	0.0	153001402W5
8	2	688661.9	567480.4	1496.5	0.0	90.0	3190.9	0.0	100401503W5
8	3	695569.7	562554.3	1481.6	0.0	90.0	2036.0	0.0	071901402W5
8	4	696047.7	549695.0	1409.7	0.0	90.0	772.7	0.0	070701302W5
8	5	701350.9	542500.8	1442.0	0.0	90.0	3078.5	0.0	151501202W5
8	6	711962.2	545893.1	1390.0	0.0	90.0	5135.0	0.0	122601201W5
8	7	697798.5	554213.4	1366.7	0.0	90.0	4373.8	0.0	022901302W5
8	8	704369.7	555656.3	1316.4	0.0	90.0	3377.0	0.0	162501302W5
8	9	710506.7	560348.0	1239.0	0.0	90.0	3676.0	0.0	101001401W5
8	10	711165.9	566089.0	1320.3	0.0	90.0	3600.0	0.0	043501401W5
8	11	698236.5	558585.7	1409.7	0.0	90.0	1751.7	0.0	010401402W5
8	12	697566.7	565038.9	1341.1	0.0	90.0	1097.3	24.0	162901402W5
8	13	696149.2	567809.2	1420.7	0.0	90.0	1655.3	0.0	120501502W5

A: Data record type: 8 = primary drillhole record
B: Drillhole identification number
C: Easting of Drillhole Kelly Bushing
D: Northing of Drillhole Kelly Bushing
E: Elevation of Kelly Bushing
F and G: Trend and plunge of the drillhole at Kelly Bushing
H: Total depth of drillhole
I: Overburden thickness: Distance between the top of the drillhole and the top of bedrock.
J: Drillhole label or identifier

Sample Deviation Records:

A	B	C	D	E
9	7	10.0	0.0	0.0

A: Data record type: 9 = Deviation record
B: Drillhole identification number
C: Downhole depth of deviation measurement
D and E: Real numbers specifying the trend of the drillhole and its deviation from vertical.

Secondary Drillhole Intersection Records:

A	B	C	D
7	7	Bf	869.0

A: Data record type: 7 = drillhole intersection record
B: Drillhole identification number
C: Horizon code
D: Downhole depth at which the horizon is encountered

Secondary Drillhole Records:

A	B	C	D	E	F
6	7	R	867.4	201.0	29.0

A: Data Record type: 6 = dipmeter data
B: Drillhole identification number
C: Horizon code
D: Downhole depth of dipmeter measurement
E and F: Two real numbers specifying the dip direction and dip of bedding from the dipmeter log

APPENDIX 2:

Orientation density diagrams for outcrops and domain test results for domains 1 through 10:

Domain #	Test #	1	2	3	4	5	6	Cylindricity
2		A	A	A	R		A	sub-cylindrical
3		A	A	A	R	A	A	cylindrical
4		A	A	A	R		A	sub-cylindrical
5		A	A	A	R		R	sub-cylindrical
8		A	A	A	R	A	R	sub-cylindrical
9		A	A	A	R	A	R	sub-cylindrical
10		A	R	A	A		A	non-cylindrical

Table 3: Summary of TRIPOD domain test analyses. Domains 1, 6, and 7 were rejected by test 1 and not further tested. Note: Tests #1, #4 and #5 are statistical tests, #5 (Chi-square test) is calculated only if multiple orientation readings for are available for individual outcrops. Tests #2 ,#3 and #6 are approximations based on the experience of TRIPOD's authors and Ramsay and Huber (1987). See following pages for detailed summary of individual tests.

Summary of Domain Test Results for Domain 1:

The vertices of the domain are:
694204. 531495.
699894. 531496.
697175. 542947.
696079. 549675.
695057. 552269.
689839. 550730.
692367. 539582.
The line dividing the domain is defined by the endpoints:
692367. 539582. 697623. 541058.
1. Woodcocks (1977) method suggests that the normals to the folded surface form a cluster.
Dip-direction & dip of mean orientation of cluster: 260.1 61.9

Summary of Domain Test Results for Domain 2:

The vertices of the domain are:
699894. 531496.
703055. 531499.
702000. 535350.
700405. 543838.
699068. 553466.
695057. 552269.
696079. 549675.
697175. 542974.
The line dividing the domain is defined by the endpoints:
691715. 542947. 700405. 543838.

1. Woodcocks (1977) method suggests that the normals to the folded surface form a girdle.

2. Average scatter of poles about plane perpendicular to fold axis is 6.0°
This scatter is probably OK for a cylindrical fold.

3. "Fold axes" in left/upper & right/lower subareas are:
168.8 .7 and 349.2 3.0
The angle between these "fold axes" is 3.8 deg.
This angle is probably OK for a cylindrical fold.

4. F test suggests that folding is non-cylindrical.

6. S-Poles within 10 deg of best fit plane: 90.7%.
S-Poles within 20 deg of best fit plane: 98.4%.
Folding is cylindrical (Ramsay and Huber, 1987).

4 out of 6 criteria suggest that folding is cylindrical.
Folding may be cylindrical
The best estimate of the "fold axis" is: 349.6 .9

Summary of Domain Test Results for Domain 3:

The vertices of the domain are:
703055. 531499.
715006. 531500.
715000. 557712.
700273. 554448.
699068. 553466.
700405. 543838.
702000. 535350.
The line dividing the domain is defined by the endpoints:
700405. 542338. 715002. 546458.

1. Woodcocks (1977) method suggests that the normals to the folded surface form a girdle.

2. Average scatter of poles about plane perpendicular to fold axis is 4.7
This scatter is probably OK for a cylindrical fold.

3. "Fold axes" in left/upper & right/lower subareas are:
169.6 1.0 and 347.6 .0
The angle between these "fold axes" is 2.3 deg.
This angle is probably OK for a cylindrical fold.

4. F test suggests that folding is non-cylindrical.

5. Chi-square test suggests that folding is cylindrical.

6. S-Poles within 10 deg of best fit plane: 95.0%.
S-Poles within 20 deg of best fit plane: 99.5%.
Folding is cylindrical (Ramsay and Huber, 1987).

5 out of 6 criteria suggest that folding is cylindrical.
Folding is probably cylindrical.
The best estimate of the fold axis is: 168.6 .5

Summary of Domain Test Results For Domain 4:
The vertices of the domain are:
700273. 554448.
715000. 557712.
715000. 570506.
698050. 570500.
The line dividing the domain is defined by the endpoints:
699401. 560587. 715000. 563890.

1. Woodcocks (1977) method suggests that the normals to the folded surface form a girdle.

2. Average scatter of poles about plane perpendicular to fold axis is 3.7
This scatter is probably OK for a cylindrical fold.

3. "Fold axes" in left/upper & right/lower subareas are:
348.2 1.5 and 353.8 1.4
The angle between these "fold axes" is 5.6 deg.
This angle is probably OK for a cylindrical fold.

4. F test suggests that folding is non-cylindrical.

6. S-Poles within 10 deg of best fit plane: 97.1%.
S-Poles within 20 deg of best fit plane: 100.0%.
Folding is cylindrical (Ramsay and Huber, 1987).

4 out of 6 criteria suggest that folding is cylindrical.
Folding may be cylindrical
The best estimate of the "fold axis" is: 350.4 1.3

Summary of Domain Test Results For Domain 5:

The vertices of the domain are:
694772. 559679.
699402. 560587.
698050. 570500.
692496. 570500.
692100. 566750.
692900. 562750.
694197. 560658.
The line dividing the domain is defined by the endpoints:
692700. 563840. 698850. 565000.

1. Woodcocks (1977) method suggests that the normals to the folded surface form a girdle.

2. Average scatter of poles about plane perpendicular to fold axis is 7.0
This scatter is probably OK for a cylindrical fold.

3. "Fold axes" in left/upper & right/lower subareas are:
349.6 .2 and 170.7 8.5
The angle between these "fold axes" is 8.8 deg.
This angle is probably OK for a cylindrical fold.

4. F test suggests that folding is non-cylindrical.

6. S-Poles within 10 deg of best fit plane: 84.7%.
S-Poles within 20 deg of best fit plane: 99.2%.
Folding is sub-cylindrical (Ramsay and Huber, 1987).

3 out of 5 criteria suggest that folding is cylindrical.
Folding may be cylindrical
The best estimate of the "fold axis" is: 170.6 5.9

Summary of Domain Test Results For Domain 6:

The vertices of the domain are:
692550. 558860.
694772. 559679.
694197. 560658.
692900. 562750.
692100. 566750.
692496. 570500.
688297. 570500.
692110. 559954.
The line dividing the domain is defined by the endpoints:
692700. 563840. 690925. 563250.

1. Woodcocks (1977) method suggests that the normals to the folded surface form a cluster.
Dip-direction & dip of mean orientation of cluster: 260.4 62.7

Summary of Domain Test Results For Domain 7:

The vertices of the domain are:
689839. 550730.
695057. 552269.
692110. 559954.
688297. 570500.
685454. 570500.
The line dividing the domain is defined by the endpoints:
688105. 558636. 692110. 559954.

1. Woodcocks (1977) method suggests that the normals to the folded surface form a cluster.
Dip-direction & dip of mean orientation of cluster: 251.8 48.5

Summary of Domain Test Results For Domain 8:

The vertices of the domain are:
695057. 552269.
696797. 552785.
694772. 559679.
692550. 558860.
The line dividing the domain is defined by the endpoints:
695750. 556360. 693740. 555775.

1. Woodcocks (1977) method suggests that the normals to the folded surface form a girdle.

2. Average scatter of poles about plane perpendicular to fold axis is 7.2
This scatter is probably OK for a cylindrical fold.

3. "Fold axes" in left/upper & right/lower subareas are:
345.1 4.5 and 324.8 17.5
The angle between these "fold axes" is 23.7 deg.
This angle is high for a cylindrical fold.

4. F test suggests that folding is non-cylindrical.

5. Chi-square test suggests that folding is cylindrical.

6. S-Poles within 10 deg of best fit plane: 86.2%.
S-Poles within 20 deg of best fit plane: 96.6%.
Folding is sub-cylindrical (Ramsay and Huber, 1987).

3 out of 6 criteria suggest that folding is cylindrical.
Folding may be cylindrical
The best estimate of the "fold axis" is: 338.1 9.2

Summary of Domain Test Results For Domain 9:

The vertices of the domain are:
699069. 553466.
700274. 554449.
699402. 560587.
696834. 560064.
697231. 557376.
697611. 557388.
698025. 555818.
The line dividing the domain is defined by the endpoints:
697181. 557617. 699765. 558083.
1. Woodcocks (1977) method suggests that the normals to the folded surface form a girdle.

2. Average scatter of poles about plane perpendicular to fold axis is 8.2
This scatter is probably OK for a cylindrical fold.

3. "Fold axes" in left/upper & right/lower subareas are:
173.9 7.3 and 172.1 14.4
The angle between these "fold axes" is 7.3 deg.
This angle is probably OK for a cylindrical fold.

4. F test suggests that folding is non-cylindrical.

5. Chi-square test suggests that folding is cylindrical.

6. S-Poles within 10 deg of best fit plane: 78.7%.
S-Poles within 20 deg of best fit plane: 97.2%.
Folding is sub-cylindrical (Ramsay and Huber, 1987).

4 out of 6 criteria suggest that folding is cylindrical.
Folding may be cylindrical
The best estimate of the "fold axis" is: 173.1 12.4

Summary of Domain Test Results For Domain 10:

The vertices of the domain are:
696797. 552786.
699069. 553466.
698025. 555818.
697611. 557388.
697231. 557376.
696834. 560064.
694773. 559679.
The line dividing the domain is defined by the endpoints:
695609. 556825. 697668. 557146.

1. Woodcocks (1977) method suggests that the normals to the folded surface form a girdle.

2. Average scatter of poles about plane perpendicular to fold axis is 13.2
This scatter is high for a cylindrical fold.

3. "Fold axes" in left/upper & right/lower subareas are:
174.8 10.2 and 175.0 13.5
The angle between these "fold axes" is 3.3 deg.
This angle is probably OK for a cylindrical fold.

4. F test suggests that folding is cylindrical.

6. S-Poles within 10 deg of best fit plane: 81.3%.
S-Poles within 20 deg of best fit plane: 89.6%.
Folding is non-cylindrical (Ramsay and Huber, 1987).

3 out of 6 criteria suggest that folding is cylindrical.
Folding may be cylindrical
The best estimate of the "fold axis" is: 175.3 12.9

Domain 1 Density Diagram
EQUAL-AREA PROBABILITY DIAGRAM. N = 258
CONCENTRATION PARAMETER = 100
CONTOURS ARE DENSITIES EXPRESSED A
MULTIPLES OF A UNIFORM DENSITY.
CONTOURS AT DENSITIES OF
2 5 10

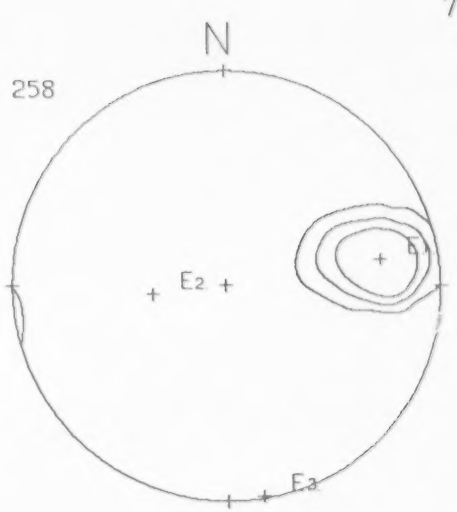

TREND	PLUNGE	EVALS/258
80.1	28.1	0.9100
263.1	61.8	0.0800
170.7	1.2	0.0100

Domain 2 Density Diagram
EQUAL-AREA PROBABILITY DIAGRAM. N = 257
CONCENTRATION PARAMETER = 100
CONTOURS ARE DENSITIES EXPRESSED A
MULTIPLES OF A UNIFORM DENSITY.
CONTOURS AT DENSITIES OF
2 5 10

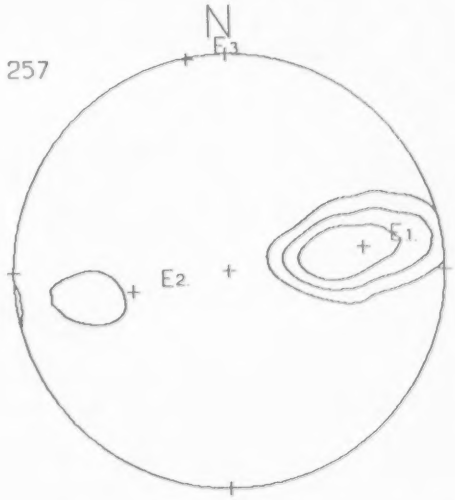

TREND	PLUNGE	EVALS/257
80.2	37.2	0.8000
258.4	52.8	0.1900
349.5	0.9	0.0100

Domain 3 Density Diagram
EQUAL-AREA PROBABILITY DIAGRAM. N = 584
CONCENTRATION PARAMETER = 100
CONTOURS ARE DENSITIES EXPRESSED A
MULTIPLES OF A UNIFORM DENSITY.
CONTOURS AT DENSITIES OF
2 5 10

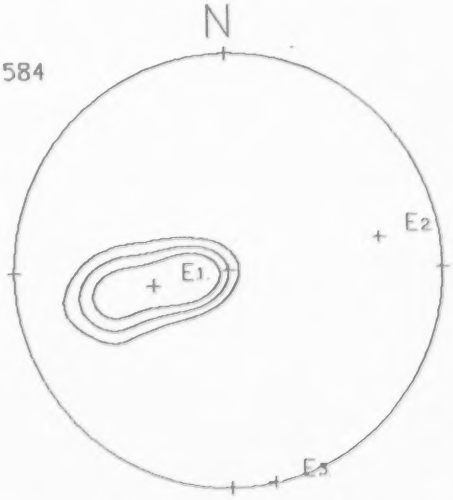

TREND	PLUNGE	EVALS/584
259.6	61.0	0.8900
78.3	29.0	0.1000
168.6	0.5	0.0100

Domain4 Density Diagram
EQUAL-AREA PROBABILITY DIAGRAM. N = 205
CONCENTRATION PARAMETER = 100
CONTOURS ARE DENSITIES EXPRESSED A
MULTIPLES OF A UNIFORM DENSITY.
CONTOURS AT DENSITIES OF
2 5 10

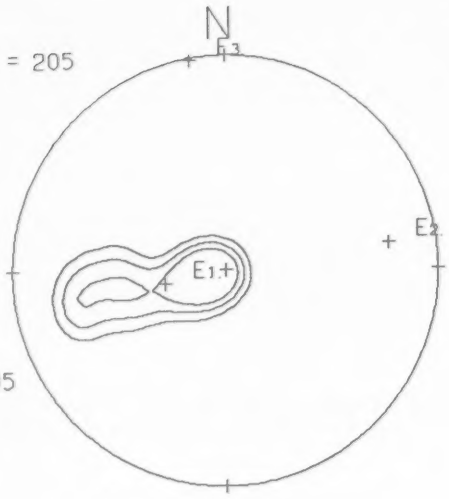

TREND	PLUNGE	EVALS/205
257.5	66.5	0.8800
81.0	23.5	0.1100
350.4	1.3	0.0000

Domain 5 Density Diagram
EQUAL-AREA PROBABILITY DIAGRAM. N = 118
CONCENTRATION PARAMETER = 100
CONTOURS ARE DENSITIES EXPRESSED A
MULTIPLES OF A UNIFORM DENSITY.
CONTOURS AT DENSITIES OF
2 5 10

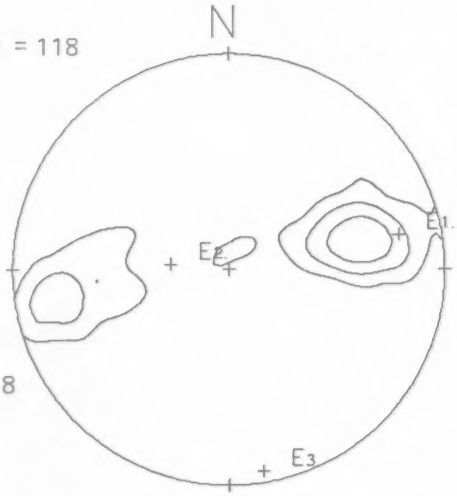

TREND	PLUNGE	EVALS/118
78.3	20.9	0.6500
275.5	68.2	0.3300
170.6	5.9	0.0100

Domain 6 Density Diagram
EQUAL-AREA PROBABILITY DIAGRAM. N = 28
CONCENTRATION PARAMETER = 100
CONTOURS ARE DENSITIES EXPRESSED A
MULTIPLES OF A UNIFORM DENSITY.
CONTOURS AT DENSITIES OF
2 5 10

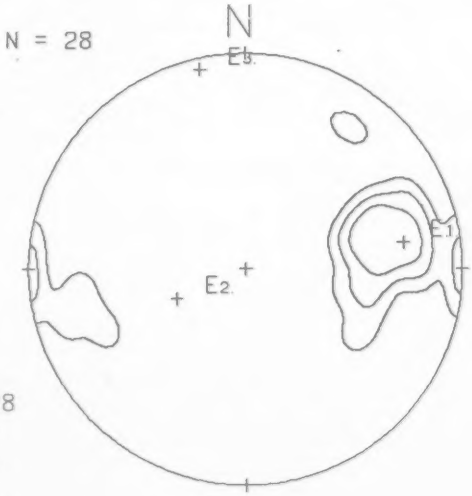

TREND	PLUNGE	EVALS/28
80.4	27.3	0.8400
246.5	62.0	0.1200
347.4	5.7	0.0400

Domain 7 Density Diagram
EQUAL-AREA PROBABILITY DIAGRAM. N = 101
CONCENTRATION PARAMETER = 100
CONTOURS ARE DENSITIES EXPRESSED A
MULTIPLES OF A UNIFORM DENSITY.
CONTOURS AT DENSITIES OF
2 5 10

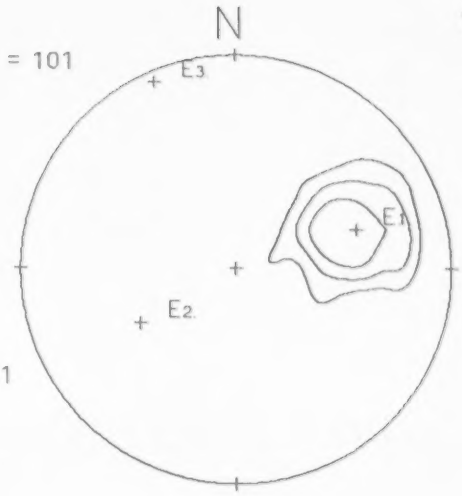

TREND	PLUNGE	EVALS/101
71.8	41.5	0.8400
240.1	47.9	0.1300
336.6	5.8	0.0300

Domain 8 Density Diagram
EQUAL-AREA PROBABILITY DIAGRAM. N = 29
CONCENTRATION PARAMETER = 100
CONTOURS ARE DENSITIES EXPRESSED A
MULTIPLES OF A UNIFORM DENSITY.
CONTOURS AT DENSITIES OF
2 5 10

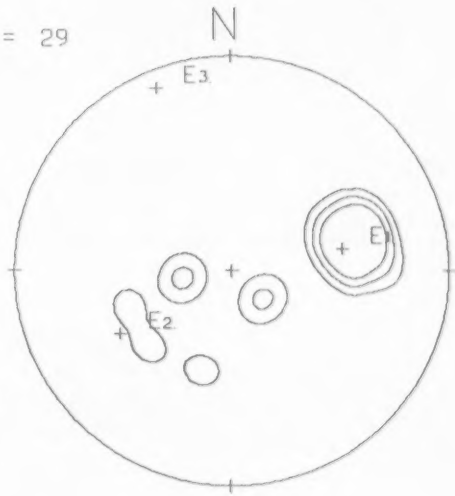

TREND	PLUNGE	EVALS/29
78.3	47.6	0.8100
240.0	40.9	0.1800
338.1	9.2	0.0200

Domain 9 Density Diagram
EQUAL-AREA PROBABILITY DIAGRAM. N = 108
CONCENTRATION PARAMETER = 100
CONTOURS ARE DENSITIES EXPRESSED A
MULTIPLES OF A UNIFORM DENSITY.
CONTOURS AT DENSITIES OF
2 5 10

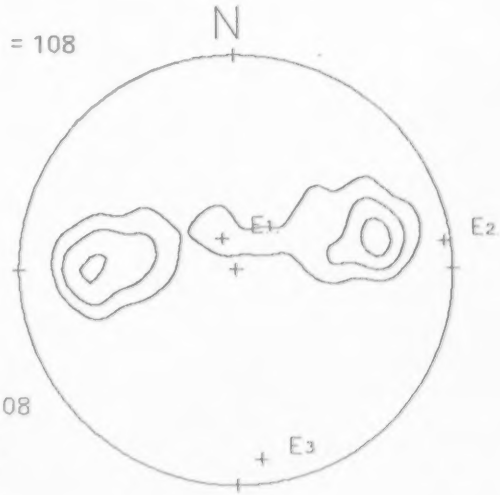

TREND	PLUNGE	EVALS/108
337.0	77.1	0.5000
82.3	3.5	0.4800
173.1	12.4	0.0200

Domain 10 Density Diagram
EQUAL-AREA PROBABILITY DIAGRAM. N = 48
CONCENTRATION PARAMETER = 100
CONTOURS ARE DENSITIES EXPRESSED A
MULTIPLES OF A UNIFORM DENSITY.
CONTOURS AT DENSITIES OF
2 5 10

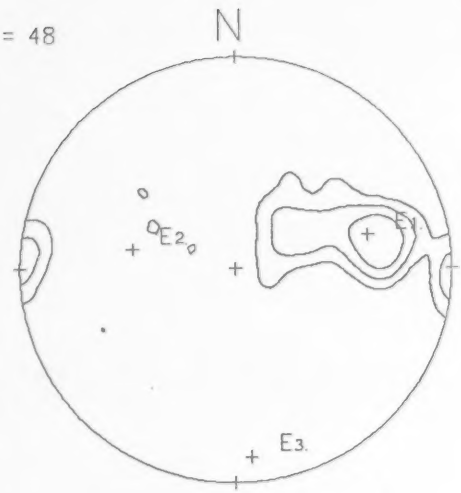

TREND	PLUNGE	EVALS/48
75.3	37.1	0.7100
281.1	50.0	0.2400
175.3	12.9	0.0500

APPENDIX 3

Statistical Curvature Analysis Technique (SCAT) results for Wells 15-15-12-2W5 and 16-25-13-2W5.

Statistical Curvature Analysis Technique (SCAT) plots display various components of dipmeter data. The interpretation and construction of these plots are summarized by Bengston (1981, 1982). These plots are very useful in the interpretation of dipmeter data. The plots may be used to identify fault surfaces, folded strata (including the position of axial planes) and unconformities. The various SCAT plots are:

A: Azimuth versus Depth plot; displays azimuth of dip (x axis) versus depth (y axis).

B: Dip versus Depth plot; displays dip (x axis) versus depth (y axis).

C: Azimuth versus Dip: displays azimuth of dip (x axis) versus dip (y axis) for a specified interval.

D: Transverse Dip Component plot: Individual dipmeter orientations are projected onto a plane of cross section which is parallel to the direction of maximum structural change (Transverse direction). The dip component (x axis) is either positive or negative, depending on whether the dip is to the left or right in the plane of cross section (Bengston, 1981). The dip component is plotted versus depth (y axis)

E: Longitudinal Dip Component plot: This plot is similar to the Transverse component plot, except the plane of cross section is the direction of least structural change (normal to the Transverse direction).

Note: transverse and longitudinal directions are usually derived from plots A, B and C.

F: Vector plot: Plane of Cross section is parallel to the transverse direction and display traces of dipmeter readings.

G: Orientation Density diagrams: Contoured orientation diagrams generated for specific intervals within the well. All orientation diagrams are contoured equal area probability density diagrams. Contours are densities expressed as multiples of a uniform density. Contours are at densities of 2, 5 and 10%. Eigen vectors and eigen values accompany each plot.

SCAT plots for Well 16-15-13-2W5:

The high degree of scatter for the dipmeter data for this well limited the amount of useful information that could be derived from the SCAT plots. All fault contacts for this well were picked from well logs: the dipmeter data did not permit positive identification of fault surfaces. The orientations of strata in the hangingwall of these faults are summarized below. Faults 2 and 3 are combined to form one set of SCAT plots. The scatter of data makes interpretations based on these data very suspect.

Summary of SCAT plots:

Fault 1:

Depth: 1170 m
Mean Orientation: 117.4° 4°

Faults 2 and 3:

Depth: Fault 2; 2900 m, Fault 3; 3050 m.
Mean Orientation: 285.7° 2°

Fault 4:

Depth: Below total depth of drillhole
Mean Orientation: 245.7° 4.2°

WELL 16-25-13-2W5

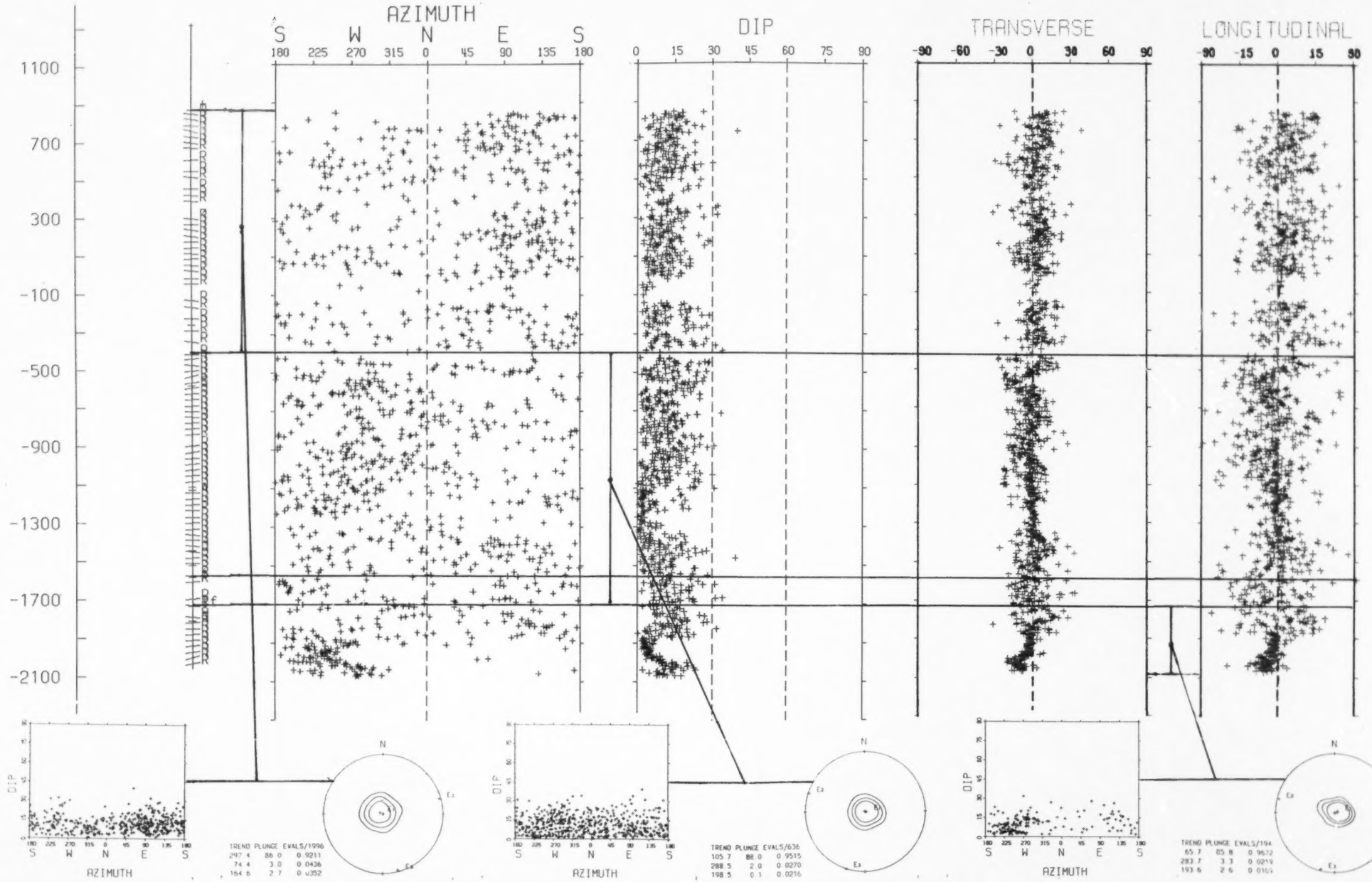

SCAT plots for Well 15-15-12-2W5:

SCAT plots for this well were very useful. Four faults were inferred from the dipmeter data. The orientations of strata in the hangingwall of each fault are summarized below. SCAT plots for strata in hangingwall of fault 2, and to a lesser degree fault 3, are typical for strata that have been folded (Bengston, 1982). The horseshoe shaped plot for strata in the hangingwall of fault 2 suggest that the fold is plunging. The orientation density diagram for these strata confirm this, the fold plunges gently toward 345.3° at 4.4°. Most of the dipmeter readings for this interval are clustered about a mean orientation (see below), but the orientation diagram suggest that the data form a weak girdle. The distribution evident on the density diagram is likely due to folding or scattered readings related to the overlying and underlying faults for this interval.

Summary of SCAT plots:

Fault 1:
Depth: 1340 m
Mean Orientation: 219.7° 8.8°

Fault 2:
Depth: 2020 m
Strata are folded: fold plunges toward 345.3° at 4.4° (E3 eigenvector).
Axial plane for the fold: Approximately 1630 m.

Note: The strata for this interval form a weak girdle. An order of magnitude difference between E1, E2 and E3 is required for data which form a girdle (Charlesworth, personal communication). A difference of this magnitude is not evident between E2 and E3, so the plunge cited for this fold may be in error.

Fault 3:
Depth: 2661 m
Mean Orientation: 250.0° 18.8°

Fault 4:
Depth: Below total depth of drillhole
Mean Orientation: 259.2° 8.4°

WELL 15-15-12-1W5

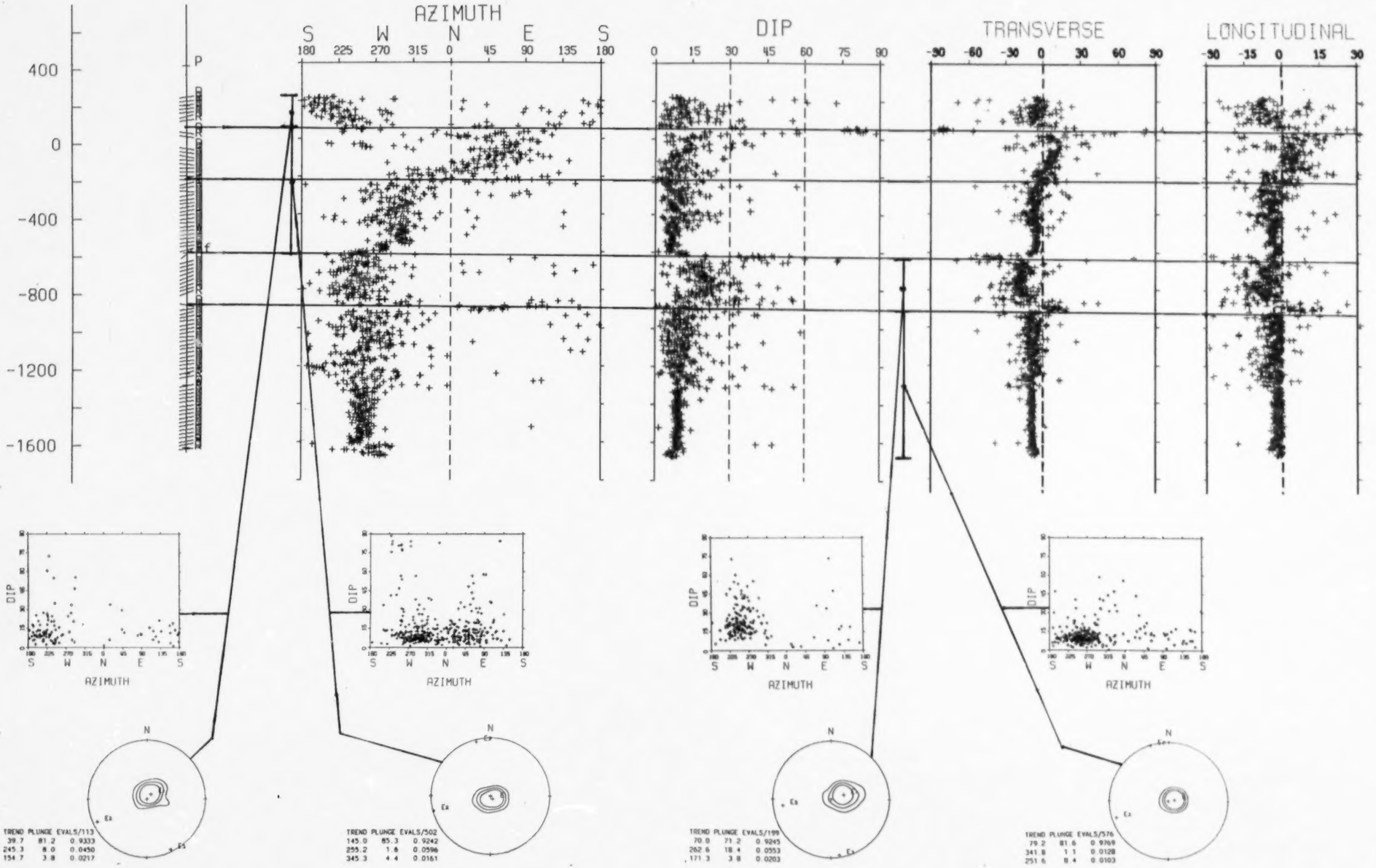

Important Note:

Figures 14, 15, 19, 20, 22, 23, 30, 31, and 32, included in the map pocket are too large to be microfilmed and may be obtained from the collections at the University of Alberta.